

*Electronic Supplementary Information*

## **Alkali Metal Ion Binding Using Cyclic Polyketones**

Narito Ozawa, Kilingaru I. Shivakumar, Muthuchamy Murugavel, Yuya Inaba, Tomoki Yoneda, Yuki Ide, Jenny Pirillo, Yuh Hijikata, and Yasuhide Inokuma\*

### **Table of contents**

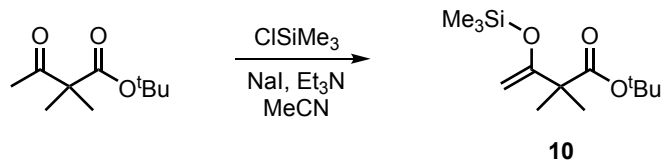
- 1. General Information**
- 2. Synthetic Procedure**
- 3. Alkali Metal Binding Experiments**
- 4. X-ray Crystallographic Analysis**
- 5. Theoretical Calculations**
- 6. Finkelstein Reaction Catalyzed by Cyclic Polyketones**
- 7. NMR Spectra**
- 8. Cartesian Coordinates of Optimized Structure**
- 9. References**

## 1. General Information

Solvents and reagents were purchased from WAKO Pure Chemical Industries Ltd., TCI Co., Ltd., or Sigma-Aldrich Co., and used without further purification unless otherwise mentioned. Compound **3**<sup>1</sup>, **4**<sup>2</sup>, **5**<sup>3</sup>, **6**<sup>2</sup>, and **9**<sup>4</sup> were prepared according to the reported procedure. All the <sup>1</sup>H and <sup>13</sup>C NMR spectra were recorded using a JEOL JMN-ECS400 spectrometer. Chemical shifts are reported in parts per million (ppm) relative to tetramethylsilane ( $\delta = 0.00$  ppm) for <sup>1</sup>H NMR and CDCl<sub>3</sub> ( $\delta = 77.16$  ppm) for <sup>13</sup>C NMR. Infrared spectra were measured using a JASCO Co. FT/IR-4600 spectrometer. Thin layered chromatography (TLC) was performed on a silica gel sheet, MERCK silica gel 60 F<sub>254</sub>. Preparative scale separations were carried out using silica gel gravity column chromatography (Wakosil® 60. 64 ~ 210  $\mu$ m) or recycling HPLC LaboACE LC-5060 equipped with two JAIGEL-2HR columns. HPLC chromatograms were recorded using a JASCO MD-2018 photodiode array detector equipped with a JASCO PU-2089 pump, JASCO AS-2059 sampler, JASCO CO-2060 column thermostat. UV-Vis absorption spectra were recorded on a Shimadzu UV-1800 spectrophotometer. Fluorescent spectra were measured on a Hitachi F-7100 spectrometer. Single crystal X-ray diffraction data were collected with Rigaku XtaLAB P200 diffractometer equipped with a PILATUS200K detector or Rigaku XtaLAB Synergy-R/DW equipped with a HyPix-6000HE detector (MoK $\alpha$  radiation  $\lambda = 0.71073$  Å). All structures were solved using a dual-space algorithm (SHELXT<sup>[5]</sup>) and refined using full-matrix least-squares method (SHELXL<sup>[6]</sup>).

## 2. Synthetic Procedure

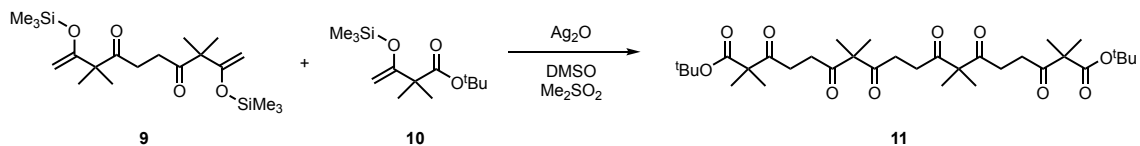
### 2-1. Synthesis of *tert*-butyl 2,2-dimethyl-3-((trimethylsilyl)oxy)but-3-enoate (**10**)



To a 500 mL three-necked round bottom flask, *tert*-butyl 2,2-dimethyl-3-oxobutanoate<sup>7</sup> (50.0 g, 268 mmol) and sodium iodide (48.3 g, 322 mmol) were added, and the flask was purged with nitrogen gas. Then acetonitrile (160 mL) and triethylamine (48.6 mL, 349 mmol) were added. The reaction mixture was cooled to 0 °C with an ice/water bath, and trimethylchlorosilane (40.9 mL, 322 mmol) was slowly added via syringe. After warming to room temperature, the reaction mixture was stirred for 3 h. After stirring, the reaction mixture was quenched by addition of water (50 mL). The mixture was transferred to a separating funnel with addition of hexane (50 mL). The aqueous layer was separated and extracted with hexane (100 mL × 3). The combined organic layer was washed with water (100 mL), dried over anhydrous sodium sulfate, and the solvent was evaporated. The crude product was purified by vacuum distillation to give compound **10** (63.6 g, 246 mmol) in 92% yield as a fraction of colorless liquid (8 Torr, 82 °C).

<sup>1</sup>H NMR (400 MHz, CDCl<sub>3</sub>, 298 K): δ 4.15 (d, *J* = 2.0 Hz, 1H, vinyl), 4.02 (d, *J* = 2.0 Hz, 1H, vinyl), 1.42 (s, 9H, *tert*-butyl), 1.26 (s, 6H, dimethylmethylenes), 0.21 (s, 9H, trimethylsilyl); <sup>13</sup>C NMR (100 MHz, CDCl<sub>3</sub>, 298 K): δ 174.9, 162.4, 86.8, 79.9, 49.1, 28.0, 24.0, 0.1; IR (ATR, neat): 2978, 1732, 1623, 1472, 1381, 1367, 1293, 1252, 1174, 1133, 1016 cm<sup>-1</sup>; HR-ESI-TOF MS: *m/z*=281.1540 (calcd. for C<sub>13</sub>H<sub>26</sub>O<sub>3</sub>Si, 281.1543 [M+Na]<sup>+</sup>); R<sub>f</sub>=0.34 (eluent: hexane/ethyl acetate = 20:1).

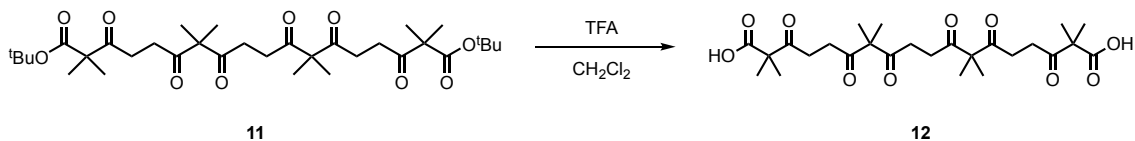
## **2-2. Synthesis of di-*tert*-butyl 2,2,7,7,12,12,17,17-octamethyl-3,6,8,11,13,16-hexaoxoocadecanedioate (11)**



To a 200 mL round bottom flask with a reflux condenser, compound **9** (7.97 g, 20.0 mmol), compound **10** (25.8 g, 100 mmol), dimethyl sulfoxide (1.99 mL, 28.0 mmol), dimethyl sulfone (39.5 g, 420 mmol), and silver(I) oxide (19.5 g, 84.0 mmol) were added. The reaction mixture was stirred at 100 °C for 2 h. After cooling to room temperature, the reaction mixture was filtrated through celite pad using dichloromethane (150 mL). The solvent was removed under reduced pressure. The mixture was transferred to a separating funnel with the addition of diethyl ether (100 mL) and brine (100 mL). The aqueous layer was extracted with diethyl ether (100 mL × 3). The combined organic layer was washed with brine (100 mL), dried over anhydrous sodium sulfate, and the solvent was evaporated. The residue was purified by silica gel column chromatography (diameter 6.0 cm, height 15 cm, eluent: hexane/ethyl acetate = 3:1). The fraction of compound **11** was solidified at low temperature, then filtrated and washed with cold hexane to afford white solid **11** (2.22 g, 3.56 mmol, yield 18%).

<sup>1</sup>H NMR (400 MHz, CDCl<sub>3</sub>, 298 K): δ 2.80 (m, 4H, ethylene), 2.73 (s, 4H, methylene), 2.71 (m, 4H, ethylene), 1.46 (s, 18H, *tert*-butyl), 1.41 (s, 12H, dimethylmethylenes), 1.34 (s, 12H, dimethylmethylenes); <sup>13</sup>C NMR (100 MHz, CDCl<sub>3</sub>, 298 K): δ 208.6, 208.2, 207.3, 172.8, 81.8, 61.9, 56.1, 32.32, 32.30, 32.0, 27.9, 22.3, 21.9; IR (ATR, neat) 2979, 1698, 1668, 1389, 1368, 1279, 1257, 1143, 1036, 1010 cm<sup>-1</sup>; HR-ESI-TOF-MS *m/z* 645.3602 (calcd. for C<sub>34</sub>H<sub>54</sub>O<sub>10</sub>, 645.3609 [M+Na]<sup>+</sup>); R<sub>f</sub> = 0.33 (eluent: hexane/ethyl acetate = 3:1); m.p. 68–70 °C.

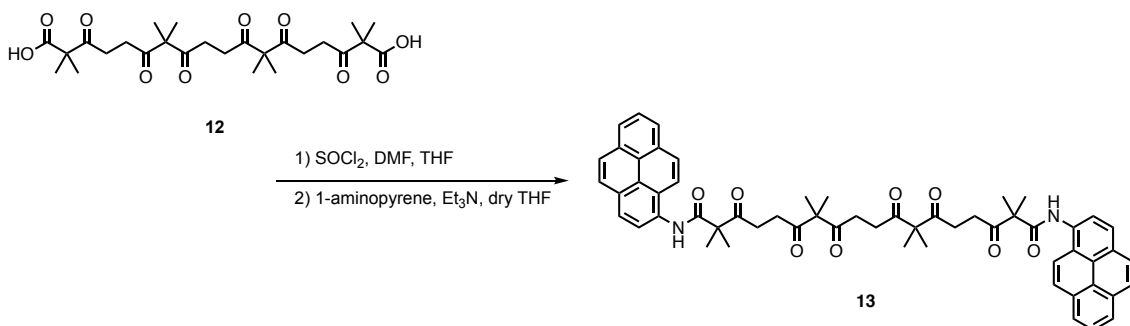
### 2-3. Synthesis of 2,2,7,7,12,12,17,17-octamethyl-3,6,8,11,13,16-hexaoxoocadecanedioic acid (12)



To a 10 mL round bottom flask, compound **11** (1.00 g, 1.61 mmol) and dichloromethane (1.2 mL) were added. The reaction solution was cooled to 0 °C and trifluoroacetic acid (2.46 mL, 32.2 mmol) was added. Thereafter, the reaction mixture was returned to room temperature and stirred for 30 min. Trifluoroacetic acid and dichloromethane were then evaporated *in vacuo* at 0 °C, and the resulting solid was filtered on a funnel with suction. The residue on a funnel was washed using hexane (4 mL) to give product **12** (735 mg, 1.44 mmol) as white solid in 90% yield. Note that compound **12** is susceptible to decarboxylation in solution at room temperature. Reaction workup should be quickly done at low temperature (~0 °C), otherwise the product will be contaminated by decarboxylated byproducts (terminal isopropyl ketones), which can be easily removed by washing a solid of **12** with diethyl ether (5mL) on a funnel.

<sup>1</sup>H NMR (CDCl<sub>3</sub>, 400 MHz): δ 10.07 (brs, 2H, -OH), 2.83 (t, 4H, ethylene, *J* = 6.0 Hz), 2.72 (t, 4H, ethylene, *J* = 6.0 Hz), 2.70 (s, 4H, methylene), 1.44 (s, 12H, dimethylmethylenes), 1.40 (s, 12H, dimethylmethylenes); <sup>13</sup>C NMR (CDCl<sub>3</sub>, 100 MHz): δ 208.7, 208.4, 207.0, 179.5, 62.0, 55.5, 32.6, 32.3, 32.1, 22.1, 21.7; IR (ATR, neat) 1715, 1697, 1469, 1387, 1369, 1292, 1186, 1067, 1021 cm<sup>-1</sup>; HR-ESI-TOF-MS *m/z* 533.2354 (calcd. for C<sub>26</sub>H<sub>38</sub>O<sub>10</sub>, 533.2357 [M+Na]<sup>+</sup>); *R*<sub>f</sub> = 0.27 (eluent: hexane/ethyl acetate/methanol = 1:1:1); m.p. 112-116 °C (decomp.).

**2-4. Synthesis of 2,2,7,7,12,12,17,17-octamethyl-3,6,8,11,13,16-hexaoxo-*N*<sup>1</sup>,*N*<sup>18</sup>-di(pyrene-1-yl)octadecanediamide (13)**



To a 10 mL round bottom flask, compound **12** (200 mg, 0.392 mmol), tetrahydrofuran (1 mL), *N,N*-dimethylformamide (10  $\mu$ L), and thionyl chloride (110  $\mu$ L, 1.57 mmol) were added. The reaction solution was stirred at room temperature for 1 h. Thionyl chloride and tetrahydrofuran were then evaporated *in vacuo* at room temperature. Then, the residue was dissolved in dry tetrahydrofuran (1 mL) under nitrogen atmosphere. After the solution was cooled to 0 °C, dry tetrahydrofuran solution (1 mL) including 1-aminopyrene (257 mg, 1.18 mmol) and triethylamine (330  $\mu$ L, 2.35 mmol) was dropwisely added. The suspension was stirred at 0 °C for 10 min. The suspension was transferred to a separating funnel with dichloromethane (15 mL) and brine (15 mL). The organic layer was separated, washed with brine (15 mL  $\times$  3), dried over anhydrous sodium sulfate, and the solvent was evaporated. The solid was washed and filtrated with toluene (15 mL) to give off-white solid **13** (260 mg, 0.286 mmol) in 73% yield.

<sup>1</sup>H NMR (400 MHz, CDCl<sub>3</sub>, 298 K):  $\delta$  8.78 (brs, 2H, N-H), 8.31 (d, 2H, *J* = 8.8 Hz, aryl), 8.13–7.93 (m, 16H, aryl), 2.92–2.89 (m, 4H, ethylene), 2.74–2.71 (m, 4H, ethylene), 2.70 (s, 4H, methylene), 1.65 (s, 12H, dimethylmethylenes), 1.36 (s, 12H, diethylmethylenes); <sup>13</sup>C NMR (100 MHz, CDCl<sub>3</sub>, 298 K):  $\delta$  211.6, 208.7, 208.3, 171.2, 131.3, 130.9, 130.5, 129.2, 127.9, 127.3, 126.9, 126.2, 125.5, 125.1, 124.7, 124.0, 122.4, 120.6, 61.9, 56.5, 32.8, 32.5, 32.4, 23.6, 21.8; IR (ATR, neat): 3310, 2987, 1699, 1654, 1515, 1503, 1464, 1365, 1278, 1184, 1034 cm<sup>-1</sup>; HR-ESI-TOF MS: *m/z* 931.3923 (calcd. for C<sub>58</sub>H<sub>56</sub>O<sub>8</sub>N<sub>2</sub>Na, 931.3929 [M+Na]<sup>+</sup>); *R*<sub>f</sub> = 0.40 (eluent: hexane/ethyl acetate = 1:2); m.p. 176–181 °C; UV-vis (dichloromethane)  $\lambda_{\text{max}}$  ( $\epsilon$ ) 278 nm (5.6  $\times$  10<sup>4</sup> L mol<sup>-1</sup> cm<sup>-1</sup>) and 342 nm (5.4  $\times$  10<sup>4</sup> L mol<sup>-1</sup> cm<sup>-1</sup>).

### UV-Vis absorption and fluorescence emission spectra of 13

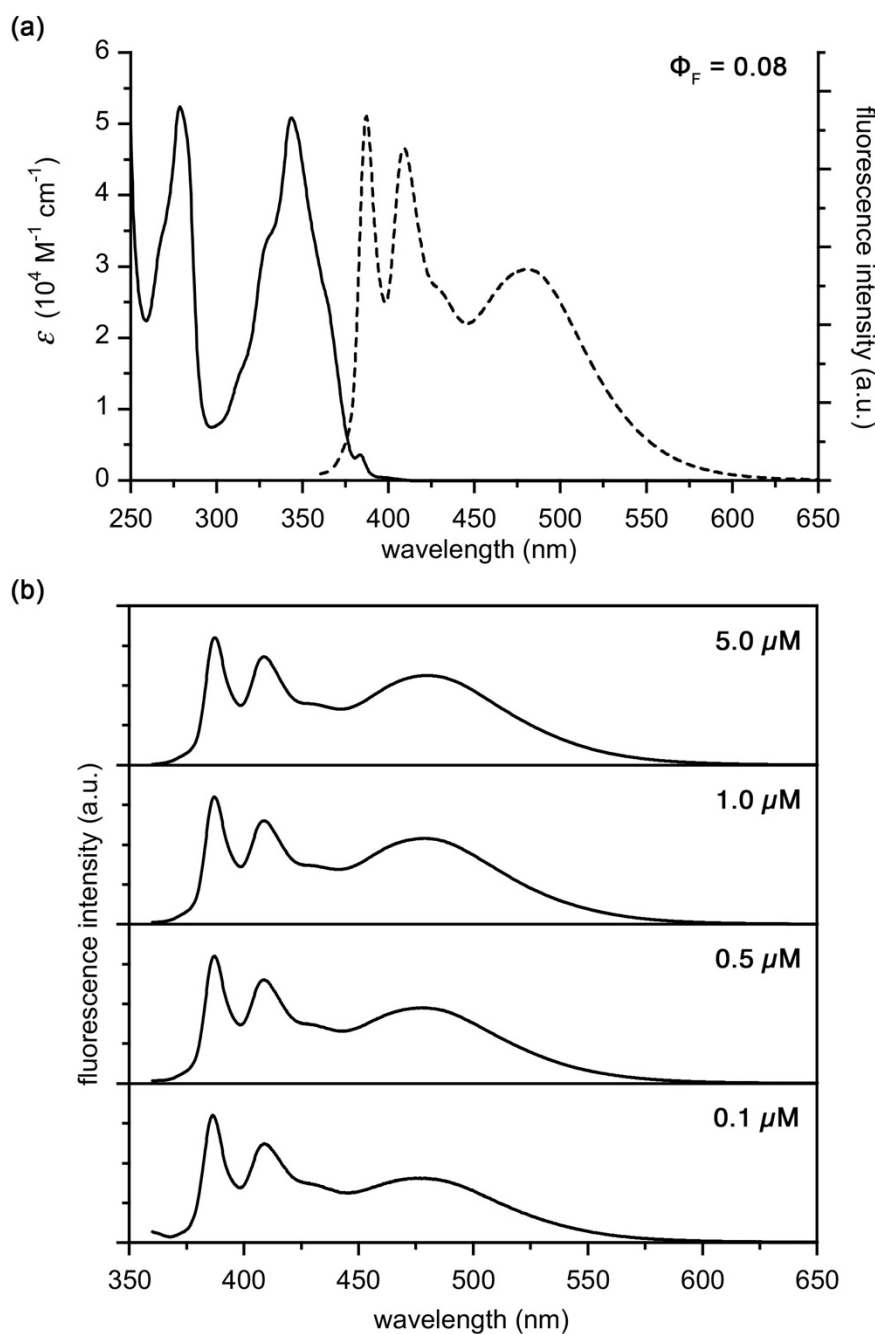
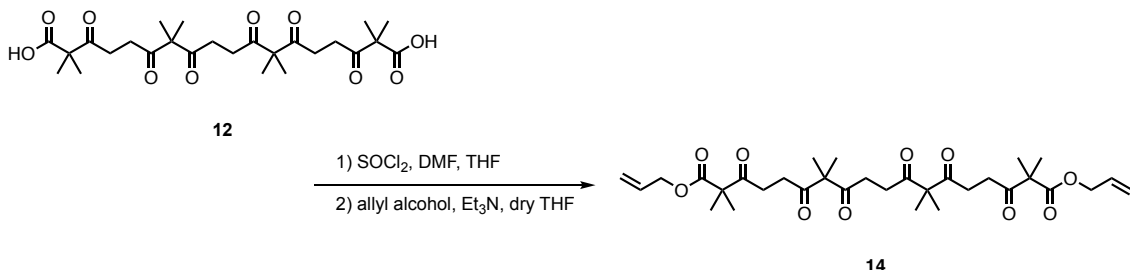


**Figure S1.** (a) UV-Vis absorption spectrum (solid line) and fluorescence emission spectrum (dotted line; excitation wavelength: 344 nm) of compound **13** in  $\text{CH}_2\text{Cl}_2$ . The relative quantum yield of **13** was determined using pyrene in  $\text{CH}_2\text{Cl}_2$ <sup>8</sup>; (b) fluorescence emission spectra of compound **13** measured under various concentrations (0.1~5.0  $\mu\text{M}$ , from bottom to top) in  $\text{CH}_2\text{Cl}_2$  (excitation wavelength: 344 nm).

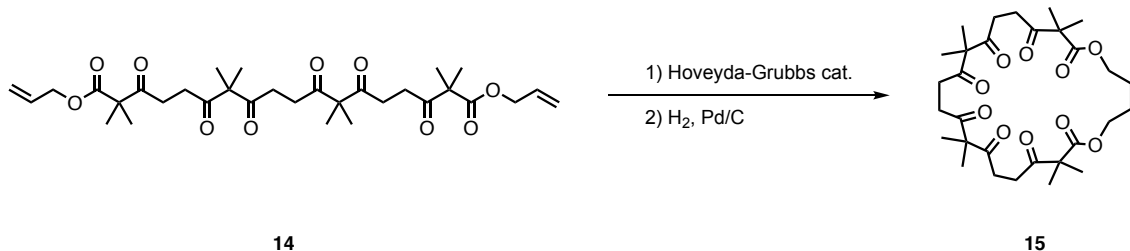
**2-5. Synthesis of diallyl 2,2,7,7,12,12,17,17-octamethyl-3,6,8,11,13,16-hexaoxoocadecanedioate (14)**



To a 50 mL round bottom flask, compound **12** (1.03 g, 2.02 mmol), tetrahydrofuran (3 mL), *N,N*-dimethylformamide (15  $\mu$ L), and thionyl chloride (1.17 mL, 16.1 mmol) were added. The reaction solution was stirred at room temperature for 1 h. Thionyl chloride and tetrahydrofuran were then evaporated *in vacuo* at room temperature. Then, dry tetrahydrofuran (3 mL) was added the flask under nitrogen gas atmosphere. After cooled to 0 °C, allyl alcohol (2.74 mL, 40.3 mmol) and triethylamine (1.69 mL, 12.1 mmol) were added dropwisely to the solution. The suspension was stirred at 0 °C for 10 min. The suspension was transferred to a separating funnel with dichloromethane (15 mL) and brine (15 mL). The organic layer was collected, washed with brine (15 mL  $\times$  3), dried over anhydrous sodium sulfate, and the solvent was evaporated. The yellow oil was separated by gel permeation chromatography using recycling HPLC. The oily fraction of compound **14** was solidified at low temperature *in vacuo* and washed with hexane (10 mL) to provide **14** (903 mg, 76%) as a white solid.

<sup>1</sup>H NMR (400 MHz, CDCl<sub>3</sub>, 298 K):  $\delta$  5.91 (ddt, *J* = 17.2, 10.4, 1.2 Hz, 2H, internal vinyl), 5.32 (ddt, *J* = 17.2, 1.8, 1.2 Hz, 2H, terminal vinyl), 5.25 (ddt, *J* = 10.4, 1.8, 1.2 Hz, 2H, terminal vinyl), 4.63 (dt, *J* = 5.6, 1.2 Hz, 4H, allyl), 2.81–2.78 (m, 4H, ethylene), 2.73–2.70 (m, 4H, ethylene), 2.72 (s, 4H, methylene), 1.42 (s, 12H, dimethylmethylenes), 1.40 (s, 12H, dimethylmethylenes); <sup>13</sup>C NMR (100 MHz, CDCl<sub>3</sub>, 298 K):  $\delta$  208.5, 208.1, 206.9, 173.3, 131.8, 118.9, 66.0, 61.9, 55.6, 32.3, 31.9, 22.3, 21.8; IR (ATR, neat): 2992, 1739, 1709, 1694, 1463, 1388, 1266, 1238, 1141, 1008 cm<sup>-1</sup>; HR-ESI-TOF MS: *m/z* 631.2977 (calcd. for C<sub>32</sub>H<sub>46</sub>O<sub>10</sub>Na, 631.2983 [M+Na]<sup>+</sup>); R<sub>f</sub> = 0.34 (eluent: hexane/ethyl acetate = 1:2); m.p. 45–47 °C.

## **2-6. Synthesis of 8,8,13,13,18,18,23,23-octamethyl-1,6-dioxacyclotetracosan-7,9,12,14,17,19,22,24-octaone (15)**



To a 200 mL two-necked round-bottom flask equipped with a magnetic stir bar and a reflux condenser, **14** (300 mg, 0.51 mmol) was added, which was followed by the addition of anhydrous and degassed dichloromethane (100 mL, 5 mM) under an inert atmosphere. Thereafter, Hoveyda-Grubbs catalyst® M720 (16 mg, 0.025 mmol) was added in one portion and the reaction mixture stirred at 50 °C for 12 h. The solvent was evaporated under reduced pressure and the residue was purified by silica gel column chromatography (diameter 3.0 cm, height 16 cm; eluent: ethyl acetate/dichloromethane/hexane = 1:2:2,  $R_f$  = 0.40) to yield 202 mg (0.36 mmol) of pure unsaturated cyclic tetramer as white solid in 70% yield.

The unsaturated cyclic tetramer (50 mg, 0.09 mmol) was added to a 10 mL round bottom flask followed by ethyl acetate (1 mL). Pd/C (5 mg, 10 wt%) was taken in a separate vial, wetted with ethyl acetate (2 mL) and the heterogenous mixture transferred to the reaction flask. Subsequently, the reaction flask was purged and stirred under H<sub>2</sub> (1 atm, balloon) atmosphere for 2 h. Upon completion, the reaction mixture was filtered. The filtrate was evaporated under reduced pressure, and purified through a silica gel column chromatography (diameter 2 cm, height 6 cm, eluent: ethyl acetate/dichloromethane/hexane = 1:2:2,  $R_f$  = 0.33) to yield 36 mg (0.064 mmol) of pure **15** as a colorless viscous oil in 72% yield.

<sup>1</sup>H NMR (CDCl<sub>3</sub>, 400 MHz): δ 4.16–4.12 (m, 4H, -OCH<sub>2</sub>-), 2.80–2.77 (m, 4H, ethylene), 2.73 (s, 4H, methylene), 2.70–2.67 (m, 4H, ethylene), 1.71–1.66 (m, 4H, -OCH<sub>2</sub>CH<sub>2</sub>CH<sub>2</sub>CH<sub>2</sub>O-), 1.401 (s, 12H, dimethylmethylenes), 1.396 (s, 12H, dimethylmethylenes); <sup>13</sup>C NMR (CDCl<sub>3</sub>, 100 MHz): δ 208.7, 207.9, 207.0, 173.5, 65.0, 62.2, 55.5, 32.43, 32.37, 32.2, 25.3, 22.2, 21.5; IR (ATR, neat); 1738, 1695, 1468, 1390, 1367, 1260, 1148, 1047, 1010 cm<sup>-1</sup>; HR-ESI-TOF MS, *m/z* 587.2812 (calcd. for C<sub>30</sub>H<sub>44</sub>O<sub>10</sub>Na, 587.2827 [M+Na]<sup>+</sup>); *R*<sub>f</sub> = 0.33 (eluent: acetate/dichloromethane/hexane = 1:2:2).

### 3. Alkali Metal Binding Experiments

#### 3-1. General procedure for NMR spectroscopic titrations

In all Alkali metal-binding processes in  $\text{CDCl}_3/\text{CD}_3\text{CN} = 9/1$  at 298 K, chemical exchanges of uncomplexed and complexed were fast with respect to the NMR timescale. Therefore all  $^1\text{H}$  NMR titration experiments were carried out by adding an Alkali metal solution dissolved in  $\text{CDCl}_3/\text{CD}_3\text{CN} = 9/1$  into a compound **3**, **4**, **5**, **6**, **13**, and **15** solution (0.5 mM) in an NMR tube using a microsyringe. Lithium salt purchased from Sigma-Aldrich was ethyl ether complex.

For the determination of association stoichiometry, Job's plot was employed.<sup>9</sup> Job's plot was conducted by changing the mole fractions of the host **3**, **4**, **5**, **6**, **13**, and **15** and guest Alkali metal ions, and the chemical shift change of host **3**, **4**, **5**, **6**, **13**, and **15** was used for the calculation.

Association constants ( $K_a$ ) were calculated from the chemical shift changes of ethylene or dimethyl proton of host **3**, **4**, **5**, **6**, **13**, and **15** by using non-linear curve-fitting method following the below equation.<sup>10</sup>

$$\Delta\delta_{\text{obs}} = \frac{\Delta\delta_{11}}{2K[H]_0} [1 + K[H]_0 + K[G]_0 - \{(1 + K[H]_0 + K[G]_0)^2 - 4K^2[H]_0[G]_0\}^{0.5}]$$

where  $\Delta\delta_{\text{obs}}$  is the chemical shift change of proton signal of ethylene or dimethyl of host **3**, **4**, **5**, **6**, **13**, and **15** at  $[G]_0$ ,  $\Delta\delta_{11}$  is the chemical shift change of host **3**, **4**, **5**, **6**, **13**, and **15** proton resonance when the host is completely complexed,  $[G]_0$  is the fixed initial concentration of Alkali metal ions, and  $[H]_0$  is initial concentration of host **3**, **4**, **5**, **6**, **13**, and **15**.

### 3-2. Complexation study of 3 and lithium salt by $^1\text{H}$ NMR spectra

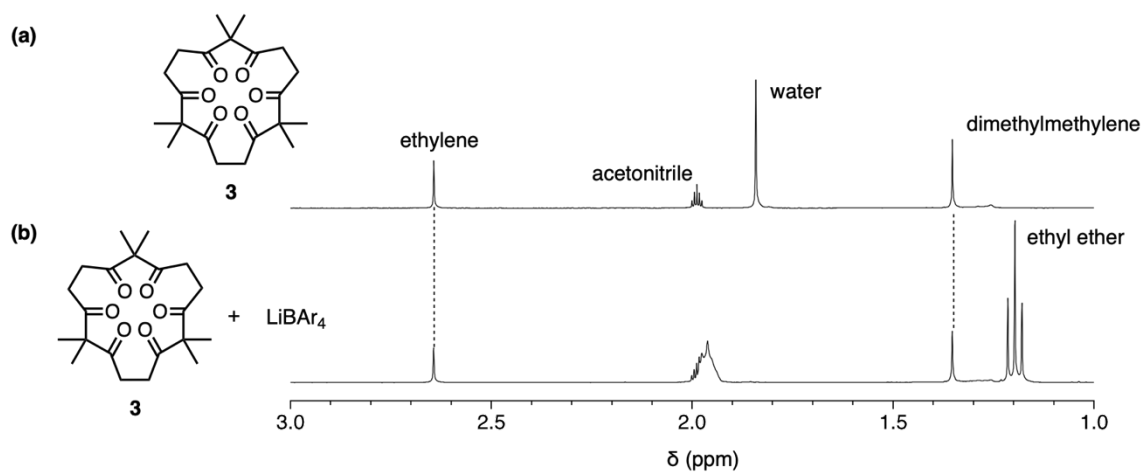


**Figure S2.** (a) Partial  $^1\text{H}$  NMR spectrum of Host 3 (0.5 mM) in  $\text{CDCl}_3/\text{CD}_3\text{CN}$  (v/v, 9:1) at 298 K; (b) Partial  $^1\text{H}$  NMR spectrum of Host 3 in the presence of  $\text{LiBAr}_4$  (5 mM, 10 eq.) in  $\text{CDCl}_3/\text{CD}_3\text{CN}$  (v/v, 9:1) at 298 K. No chemical shift changes of ethylene and dimethylmethylenes protons signals indicate no complexation between host 3 and  $\text{LiBAr}_4$ .

### 3-3. Complexation study of 3 and sodium salt by $^1\text{H}$ NMR spectra

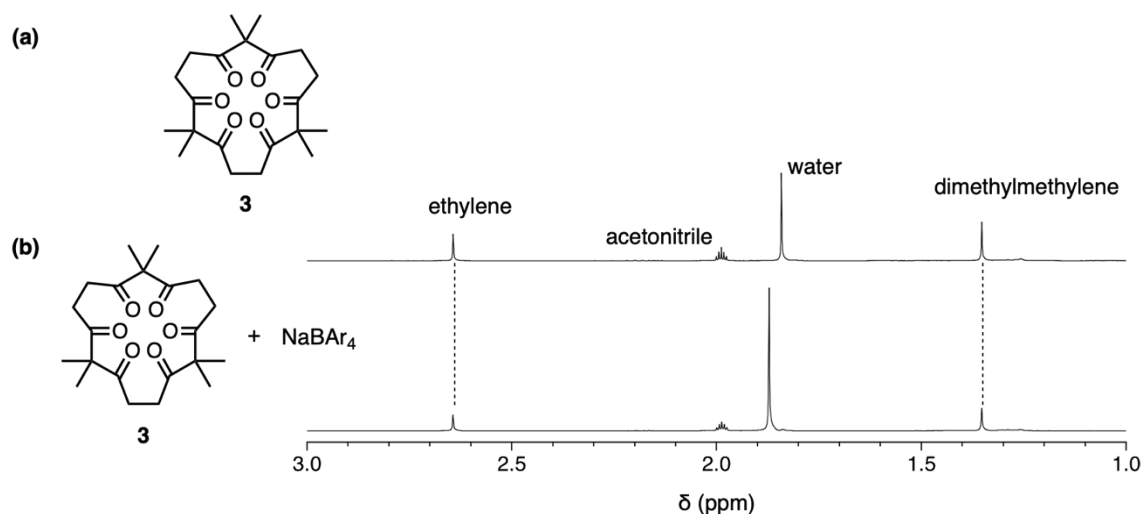


**Figure S3.** (a) Partial  $^1\text{H}$  NMR spectrum of Host 3 (0.5 mM) in  $\text{CDCl}_3/\text{CD}_3\text{CN}$  (v/v, 9:1) at 298 K; (b) Partial  $^1\text{H}$  NMR spectrum of Host 3 in the presence of  $\text{NaBAr}_4$  (5 mM, 10 eq.) in  $\text{CDCl}_3/\text{CD}_3\text{CN}$  (v/v, 9:1) at 298 K. No chemical shift changes of ethylene and dimethylmethylenes protons signals indicate no complexation between host 3 and  $\text{NaBAr}_4$ .

**3-4. Complexation study of 3 and potassium salt by  $^1\text{H}$  NMR spectra**

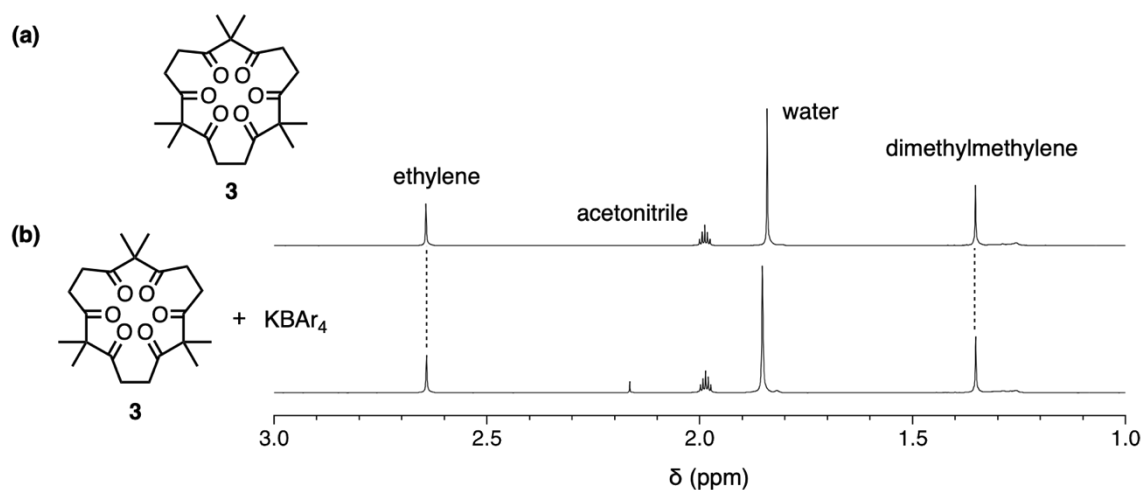


**Figure S4.** (a) Partial  $^1\text{H}$  NMR spectrum of Host 3 (0.5 mM) in  $\text{CDCl}_3/\text{CD}_3\text{CN}$  (v/v, 9:1) at 298 K; (b) Partial  $^1\text{H}$  NMR spectrum of Host 3 in the presence of KBA<sub>4</sub> (5 mM, 10 eq.) in  $\text{CDCl}_3/\text{CD}_3\text{CN}$  (v/v, 9:1) at 298 K. No chemical shift changes of ethylene and dimethylmethylenes protons signals indicate no complexation between host 3 and KBA<sub>4</sub>.

### 3-5. Complexation study of 4 and lithium salt by $^1\text{H}$ NMR spectra

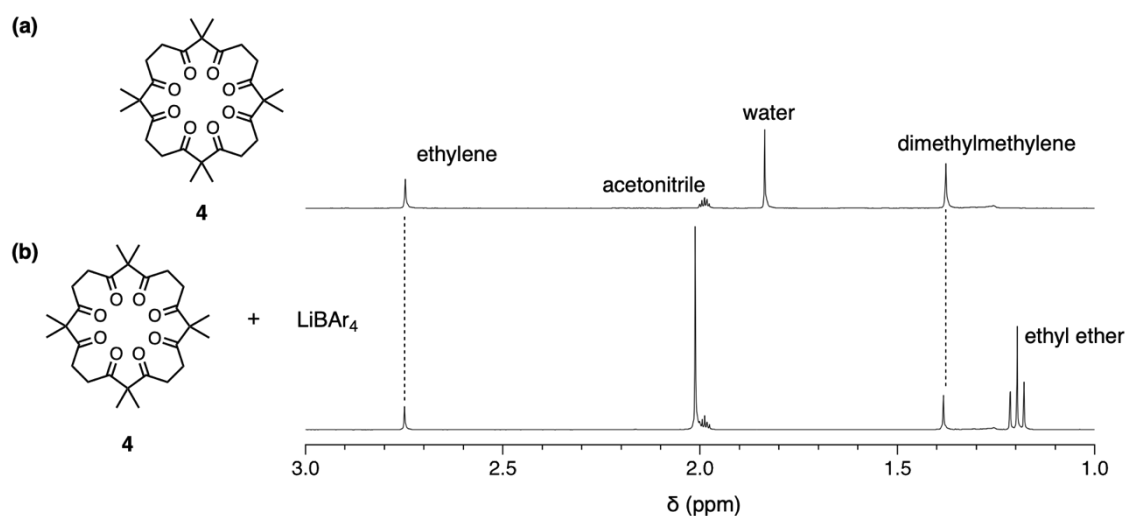


**Figure S5.** (a) Partial  $^1\text{H}$  NMR spectrum of Host **4** (0.5 mM) in  $\text{CDCl}_3/\text{CD}_3\text{CN}$  (v/v, 9:1) at 298 K; (b) Partial  $^1\text{H}$  NMR spectrum of Host **4** in the presence of  $\text{LiBAr}_4$  (5 mM, 10 eq.) in  $\text{CDCl}_3/\text{CD}_3\text{CN}$  (v/v, 9:1) at 298 K. No chemical shift changes of ethylene and dimethylmethylenes protons signals indicate no complexation between host **4** and  $\text{LiBAr}_4$ .

### 3-6. $^1\text{H}$ NMR spectroscopic titration of 4 with sodium salt

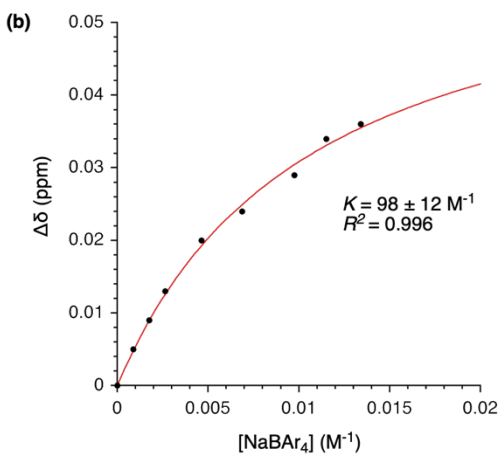
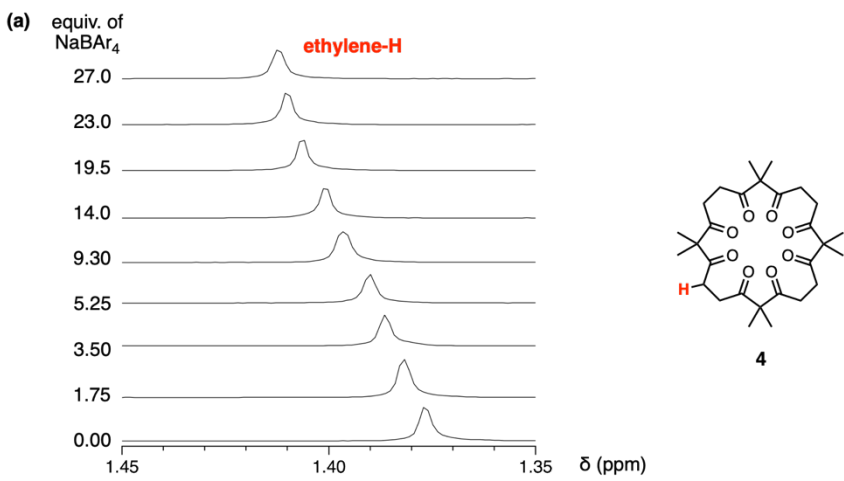
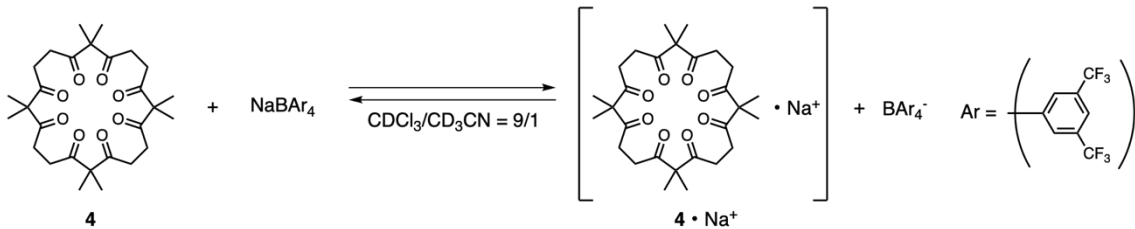


**Figure S6.** (a)  $^1\text{H}$  NMR spectra of host **4** (0.5 mM) with increasing the ratio of NaBAR<sub>4</sub> from 0.0 to 27 eq. in CDCl<sub>3</sub>/CD<sub>3</sub>CN (v/v, 9:1) at 298 K; (b) Non-linear fitting curve of  $^1\text{H}$  NMR titration.

**3-7. Complexation study of 4 and potassium salt by  $^1\text{H}$  NMR spectra**

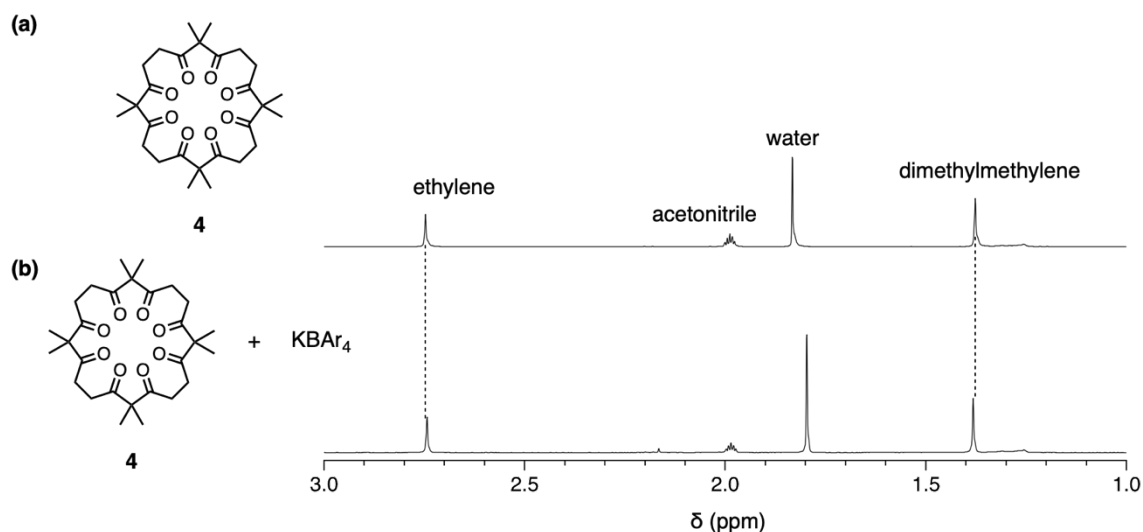


**Figure S7.** (a) Partial  $^1\text{H}$  NMR spectrum of Host **4** (0.5 mM) in  $\text{CDCl}_3/\text{CD}_3\text{CN}$  (v/v, 9:1) at 298 K; (b) Partial  $^1\text{H}$  NMR spectrum of Host **4** in the presence of  $\text{KBAr}_4$  (3 mM, 6.0 eq.) in  $\text{CDCl}_3/\text{CD}_3\text{CN}$  (v/v, 9:1) at 298 K. No chemical shift changes of ethylene and dimethylmethylenes protons signals indicate no complexation between host **4** and  $\text{KBAr}_4$ .

**3-8.  $^1\text{H}$  NMR spectroscopic titration of **5** with lithium salt**

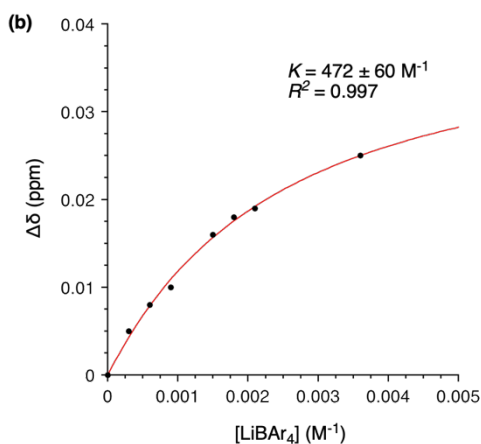
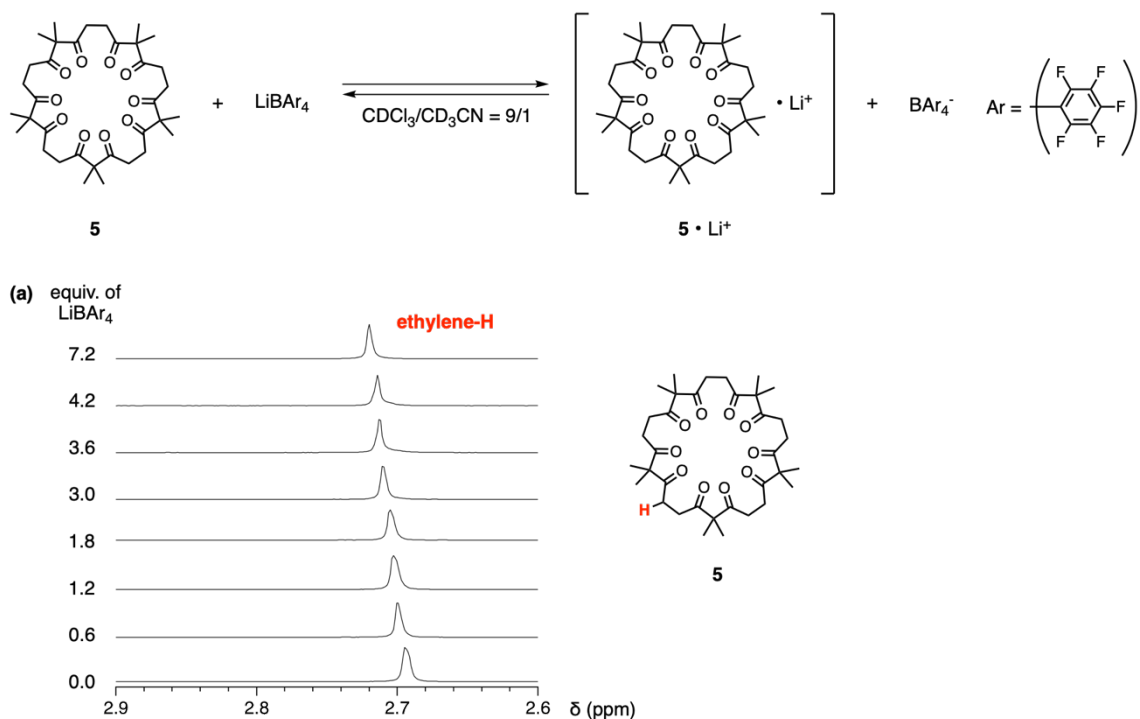


**Figure S8.** (a)  $^1\text{H}$  NMR spectra of host **5** (0.5 mM) with increasing the ratio of LiBAr<sub>4</sub> from 0.0 to 7.2 eq. in CDCl<sub>3</sub>/CD<sub>3</sub>CN (v/v, 9:1) at 298 K; (b) Non-linear fitting curve of  $^1\text{H}$  NMR titration.

**3-9.  $^1\text{H}$  NMR spectroscopic titration of **5** with sodium salt**

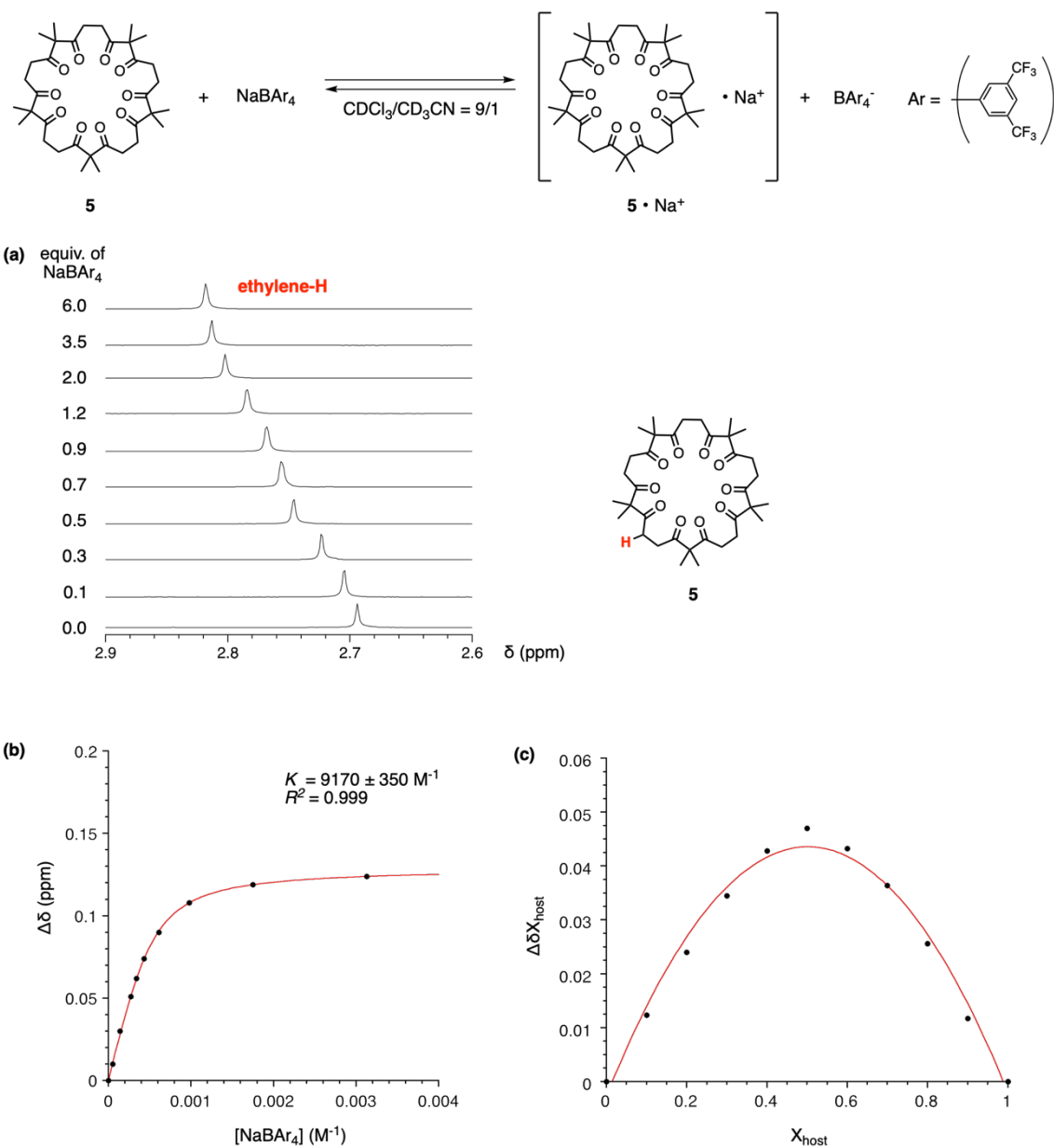


**Figure S9.** (a)  $^1\text{H}$  NMR spectra of host **5** (0.5 mM) with increasing the ratio of  $\text{NaBAr}_4$  from 0.0 to 6.0 eq. in  $\text{CDCl}_3/\text{CD}_3\text{CN}$  (v/v, 9:1) at 298 K; (b) Non-linear fitting curve of  $^1\text{H}$  NMR titration; (c) Job's plot analysis at  $[\mathbf{5}] + [\text{NaBAr}_4] = 0.5$  mM,  $X_{\text{host}} = [\mathbf{5}]/([\mathbf{5}]+[\text{NaBAr}_4])$ .

**3-10.  $^1\text{H}$  NMR spectroscopic titration of **5** with potassium salt**

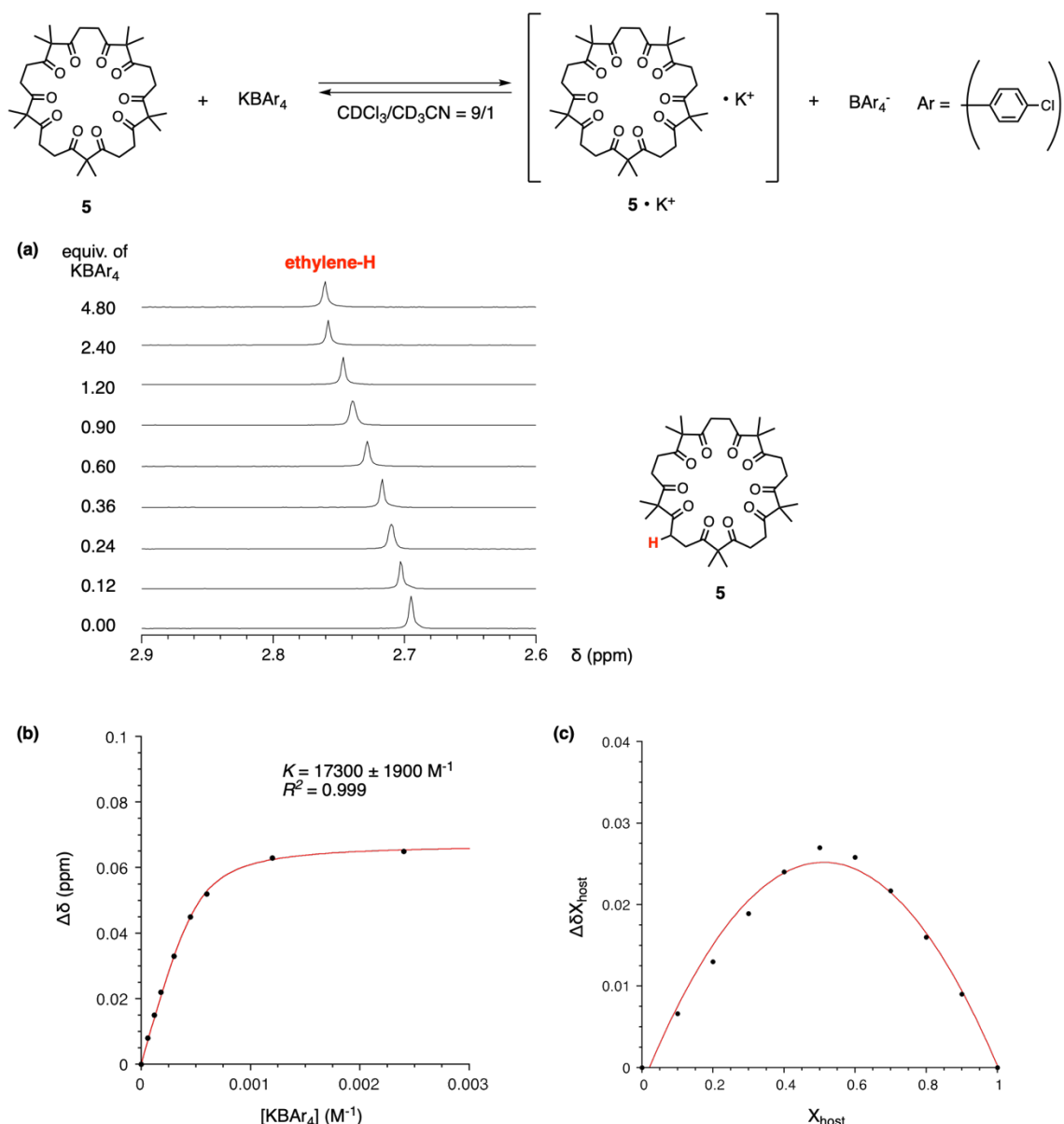


**Figure S10.** (a)  $^1\text{H}$  NMR spectra of host **5** (0.5 mM) with increasing the ratio of  $\text{KBAr}_4$  from 0.0 to 4.8 eq. in  $\text{CDCl}_3/\text{CD}_3\text{CN}$  (v/v, 9:1) at 298 K; (b) Non-linear fitting curve of  $^1\text{H}$  NMR titration; (c) Job's plot analysis at  $[\mathbf{5}] + [\text{KBAr}_4] = 0.5 \text{ mM}$ ,  $X_{\text{host}} = [\mathbf{5}] / ([\mathbf{5}] + [\text{KBAr}_4])$ .

**3-11.  $^1\text{H}$  NMR spectroscopic titration of **6** with lithium salt**

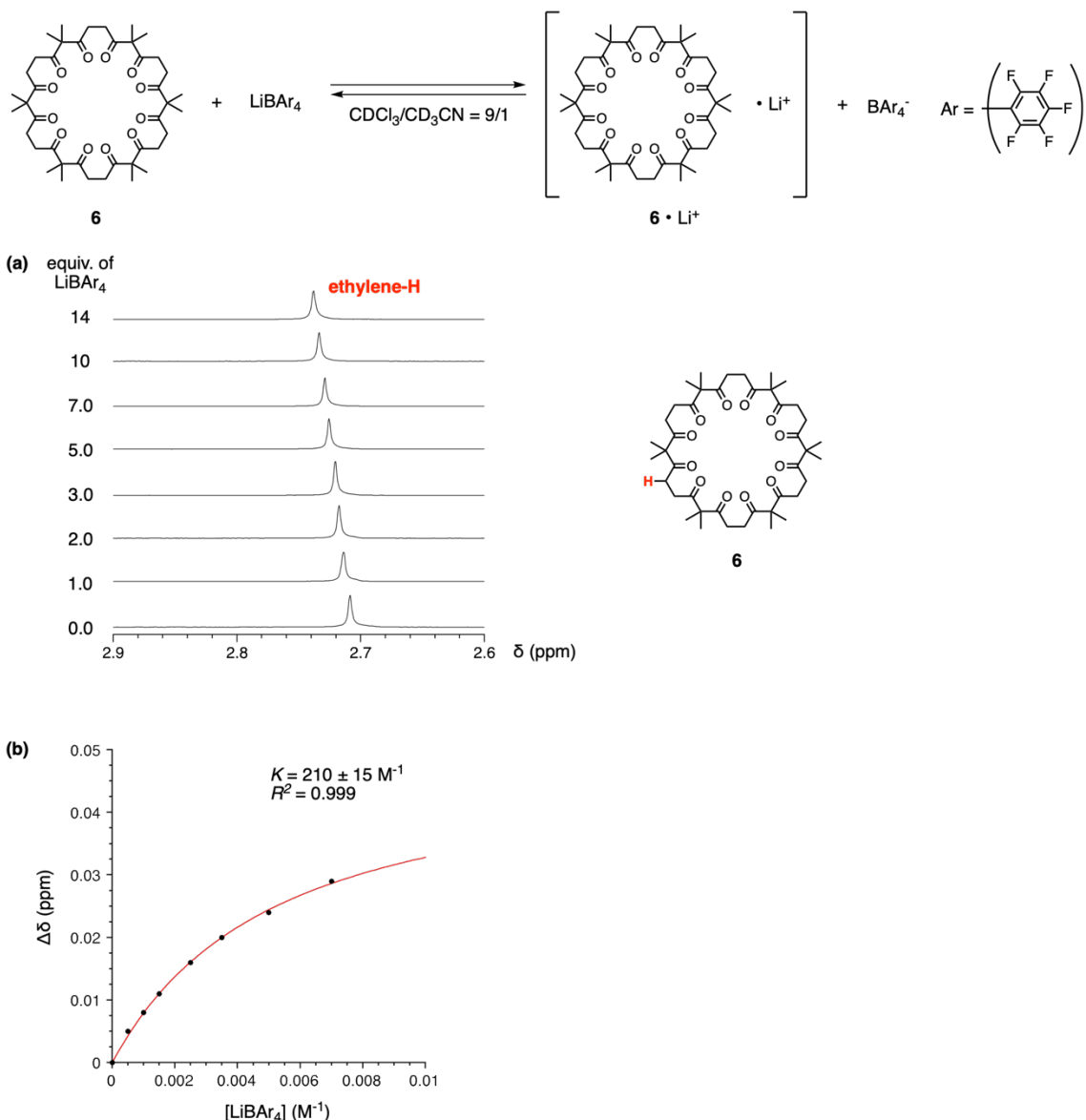


**Figure S11.** (a)  $^1\text{H}$  NMR spectra of host **6** (0.5 mM) with increasing the ratio of LiBAr<sub>4</sub> from 0.0 to 14 eq. in CDCl<sub>3</sub>/CD<sub>3</sub>CN (v/v, 9:1) at 298 K; (b) Non-linear fitting curve of  $^1\text{H}$  NMR titration.

**3-12.  $^1\text{H}$  NMR spectroscopic titration of **6** with sodium salt**

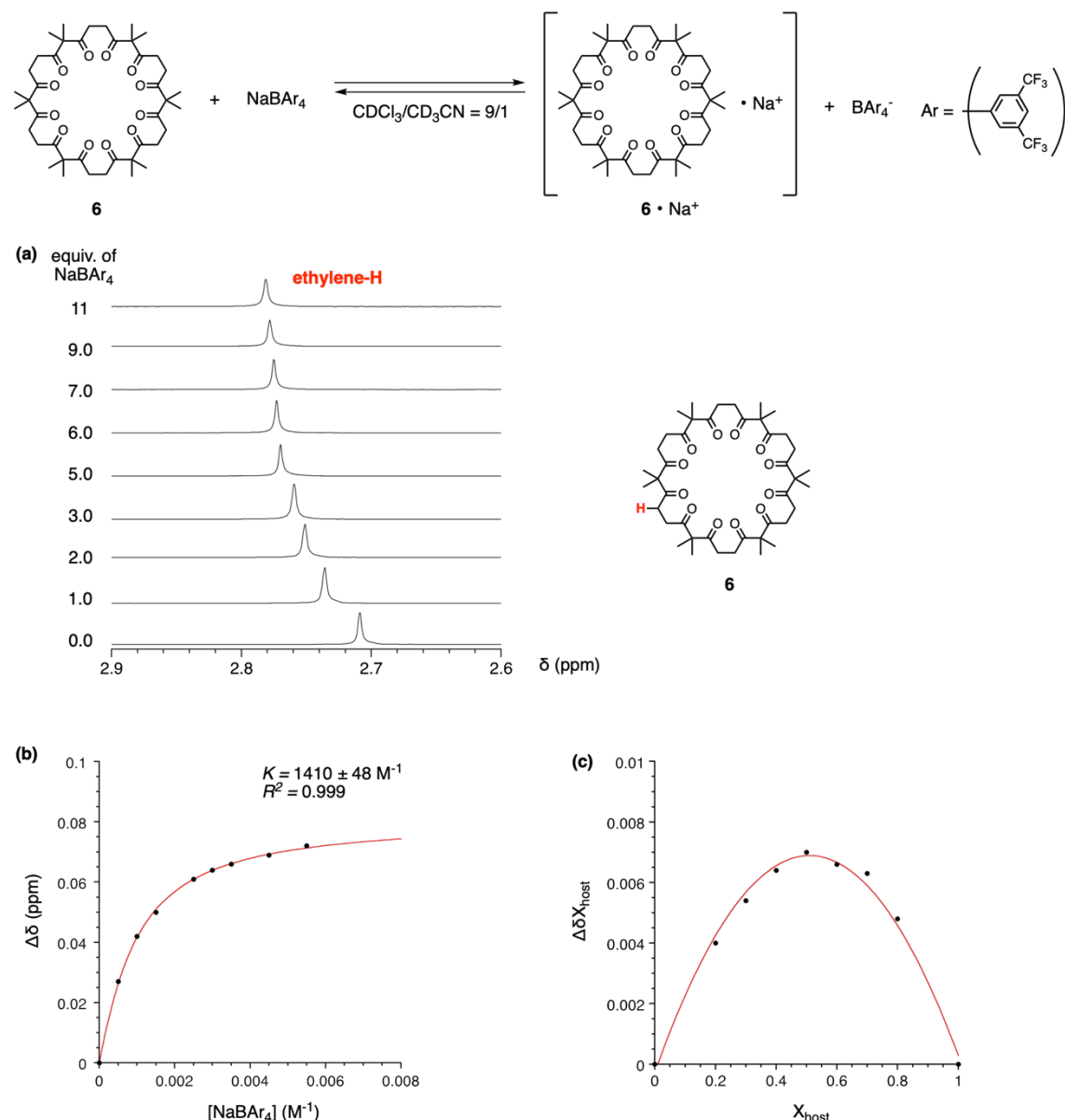


**Figure S12.** (a)  $^1\text{H}$  NMR spectra of host **6** (0.5 mM) with increasing the ratio of  $\text{NaBAr}_4$  from 0.0 to 11 eq. in  $\text{CDCl}_3/\text{CD}_3\text{CN}$  (v/v, 9:1) at 298 K; (b) Non-linear fitting curve of  $^1\text{H}$  NMR titration; (c) Job's plot analysis at  $[\mathbf{6}] + [\text{NaBAr}_4] = 0.5 \text{ mM}$ ,  $X_{\text{host}} = [\mathbf{6}]/([\mathbf{6}] + [\text{NaBAr}_4])$ .

**3-13.  $^1\text{H}$  NMR spectroscopic titration of **6** with potassium salt**

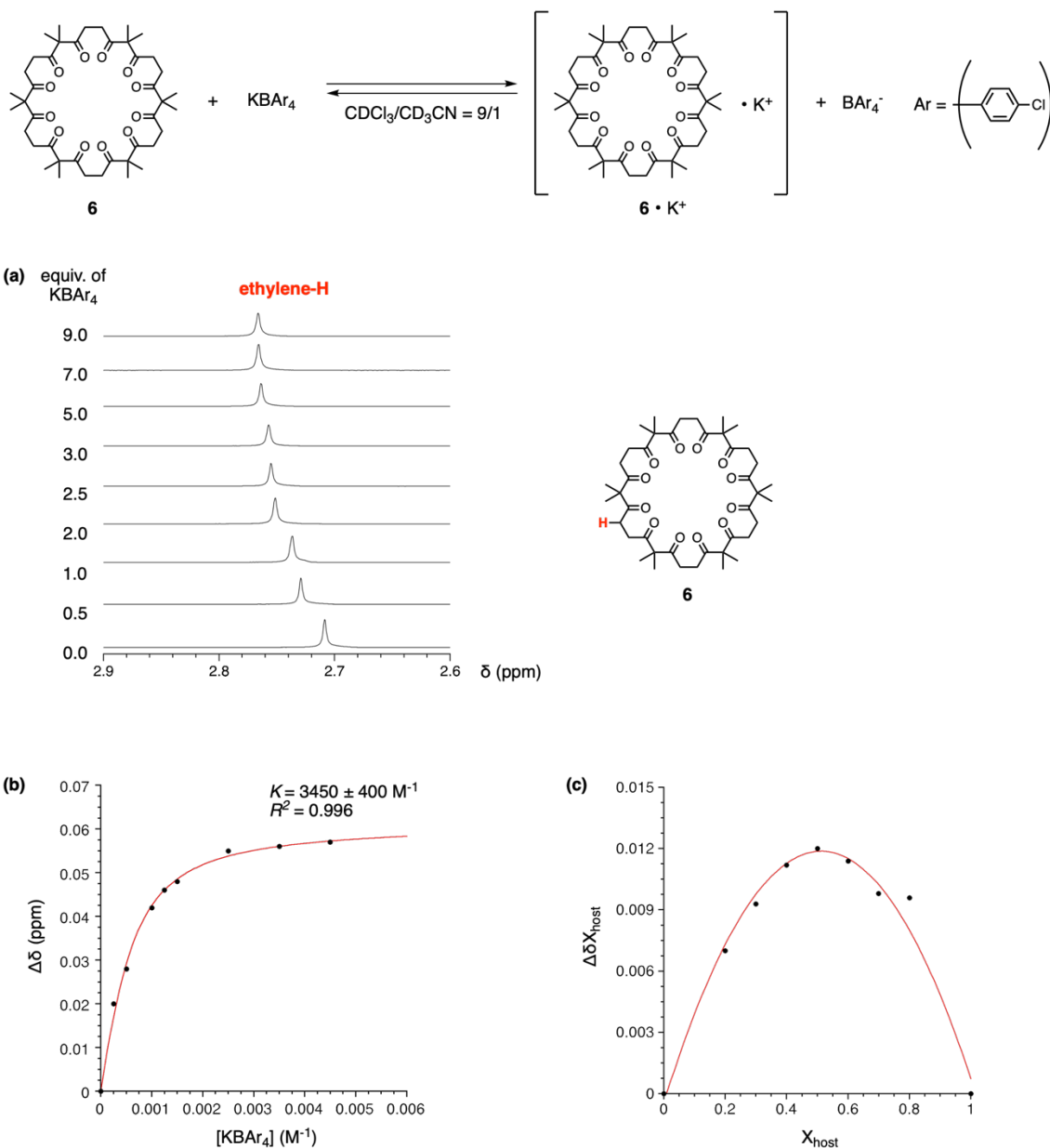


**Figure S13.** (a)  $^1\text{H}$  NMR spectra of host **6** (0.5 mM) with increasing the ratio of KBAr<sub>4</sub> from 0.0 to 9.0 eq. in CDCl<sub>3</sub>/CD<sub>3</sub>CN (v/v, 9/1) at 298 K; (b) Non-linear fitting curve of  $^1\text{H}$  NMR titration; (c) Job's plot analysis at  $[\mathbf{6}] + [\text{KBAr}_4] = 0.5 \text{ mM}$ ,  $X_{\text{host}} = [\mathbf{6}]/([\mathbf{6}]+[\text{KBAr}_4])$ .

**3-14. Complexation study if 13 and lithium salt by  $^1\text{H}$  NMR spectra**

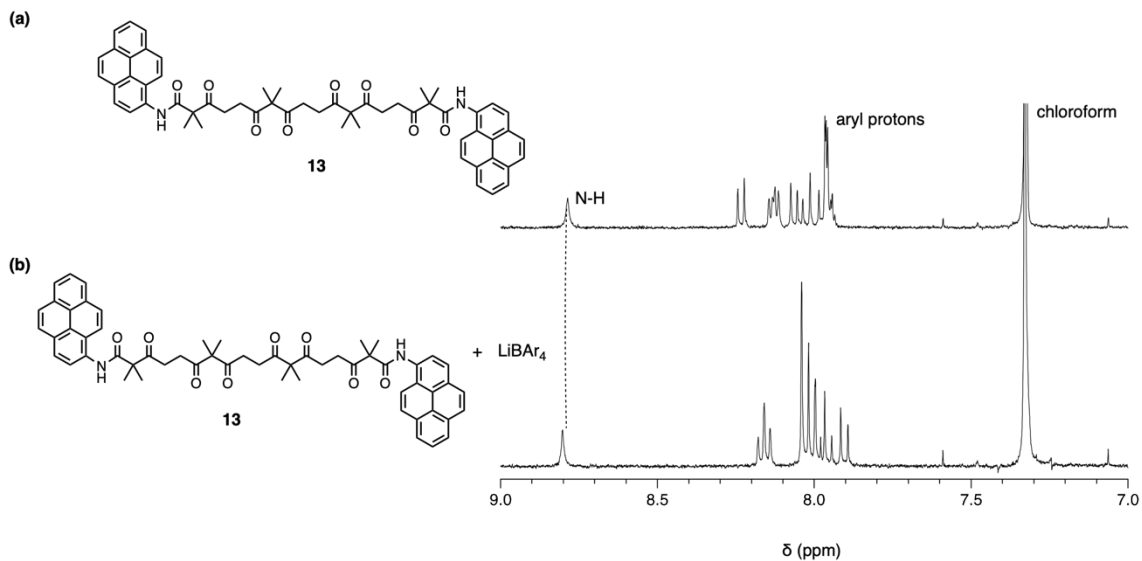


**Figure S14.** (a) Partial  $^1\text{H}$  NMR spectrum of Host **13** (0.5 mM) in  $\text{CDCl}_3/\text{CD}_3\text{CN}$  (v/v, 9:1) at 298 K; (b) Partial  $^1\text{H}$  NMR spectrum of Host **13** in the presence of  $\text{LiBAr}_4$  (4 mM, 8.0 eq.) in  $\text{CDCl}_3/\text{CD}_3\text{CN}$  (v/v, 9:1) at 298 K. No chemical shift changes of N-H protons signals indicate no complexation between host **13** and  $\text{LiBAr}_4$ .

**3-15.  $^1\text{H}$  NMR spectroscopic titration of **13** with sodium salt**

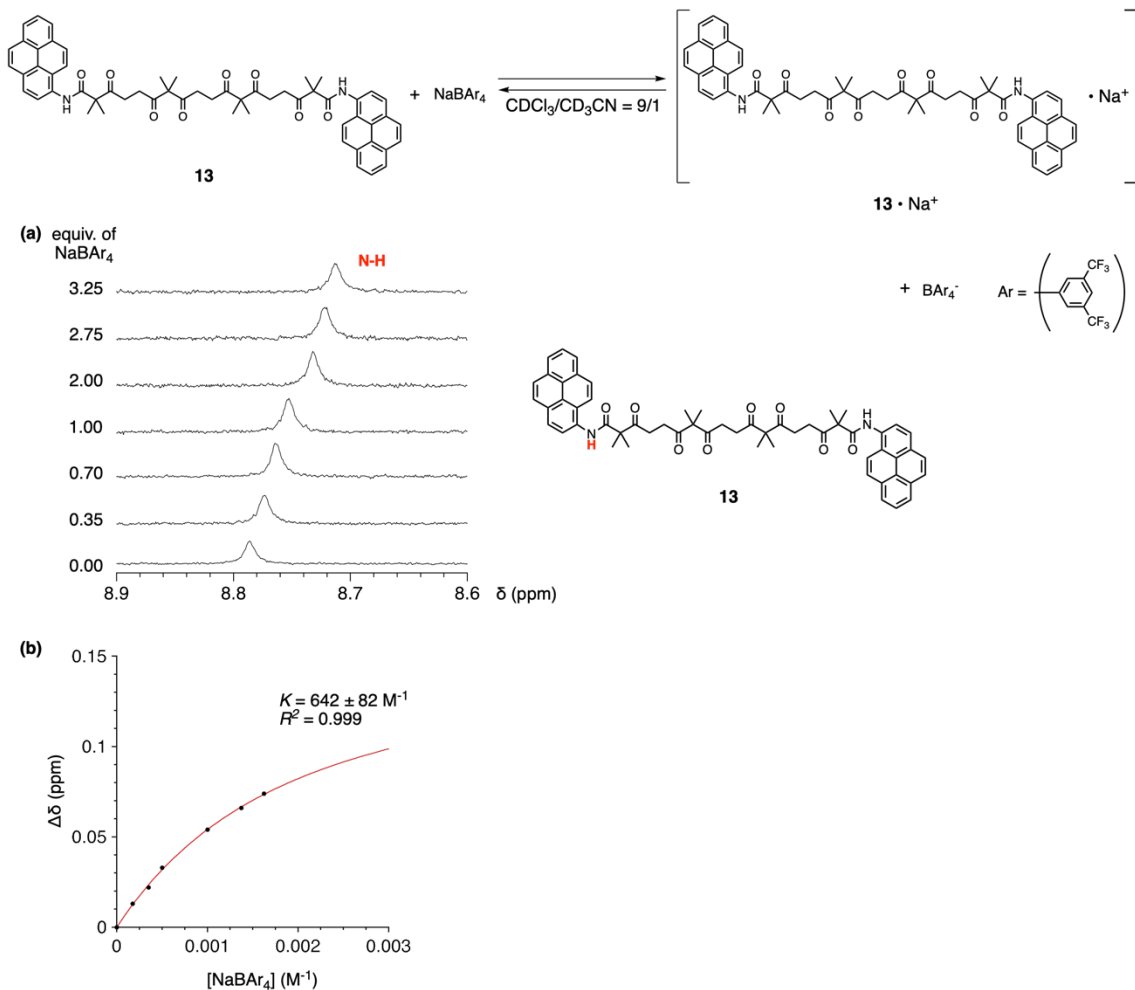


**Figure S15.** (a)  $^1\text{H}$  NMR spectra of host **13** (0.5 mM) with increasing the ratio of  $\text{NaBAr}_4$  from 0.0 to 3.75 eq. in  $\text{CDCl}_3/\text{CD}_3\text{CN}$  (v/v, 9:1) at 298 K; (b) Non-linear fitting curve of  $^1\text{H}$  NMR titration.

**3-16.  $^1\text{H}$  NMR spectroscopic titration of **13** with potassium salt**

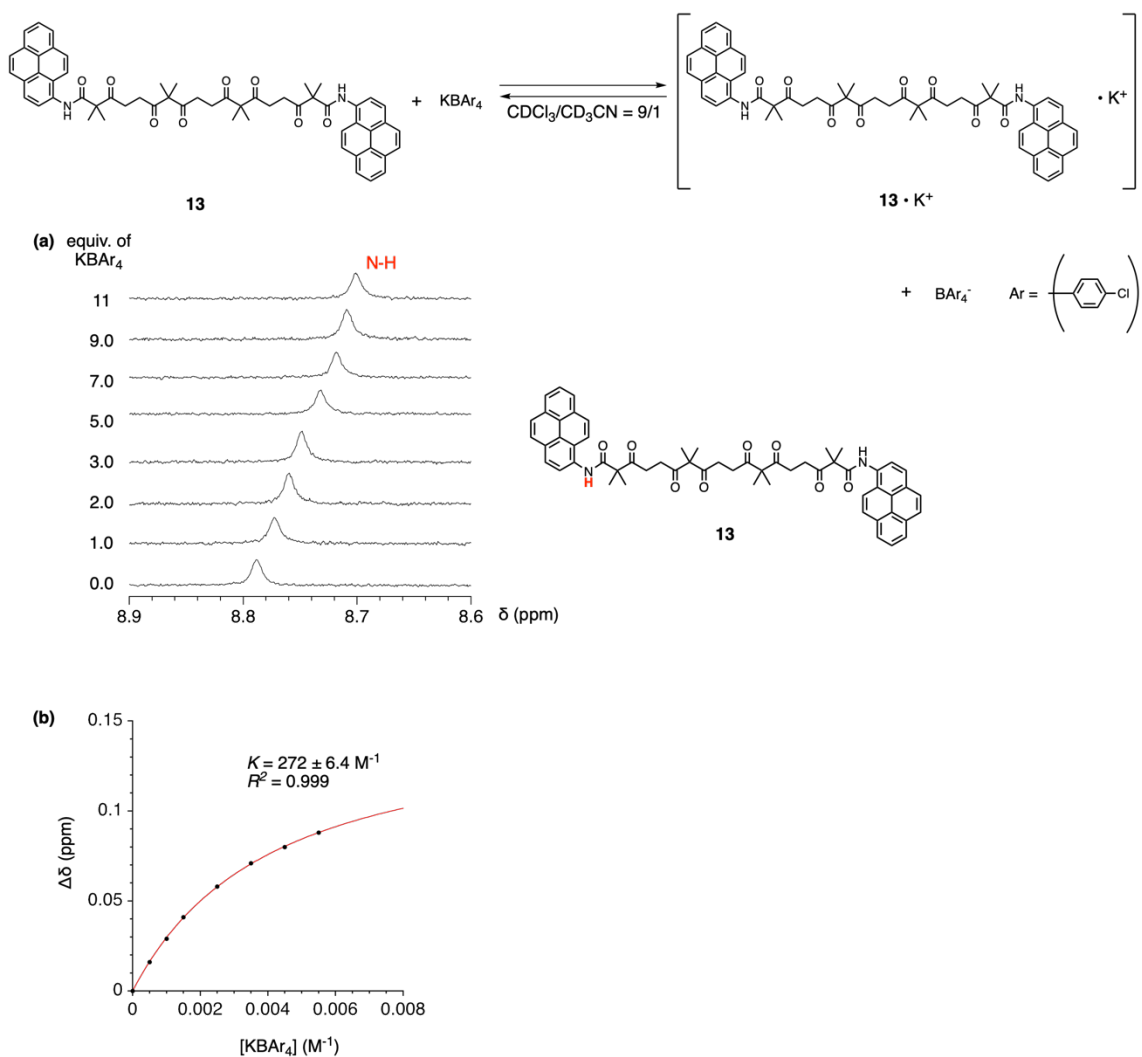


**Figure S16.** (a)  $^1\text{H}$  NMR spectra of host **13** (0.5 mM) with increasing the ratio of  $\text{KBAr}_4$  from 0.0 to 11 eq. in  $\text{CDCl}_3/\text{CD}_3\text{CN}$  (v/v, 9:1) at 298 K; (b) Non-linear fitting curve of  $^1\text{H}$  NMR titration.

**3-17. UV-Vis and fluorescence titration study for **13** and sodium salt**

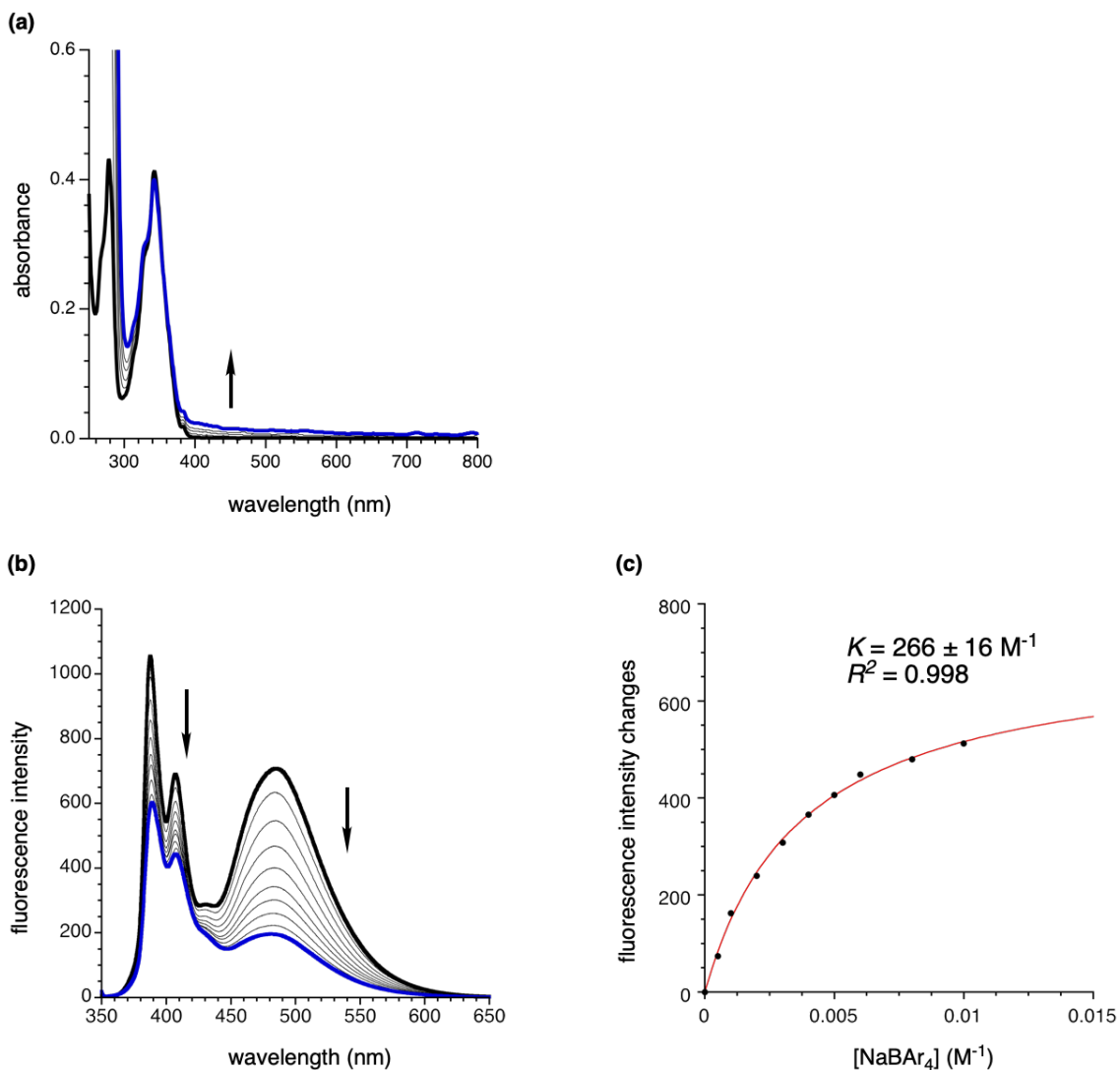


**Figure S17.** (a) UV-vis absorption spectra of **13** (10  $\mu$ M) during addition of 0.0 (black bold line), 10, 50, 100, 300 and 500 equivalents (blue bold line) of NaBAr<sub>4</sub> in CHCl<sub>3</sub>/CH<sub>3</sub>CN (v/v, 9:1); (b) fluorescence emission spectra of **13** (10  $\mu$ M) during addition of 0.0 (black bold line), 50, 100, 200, 300, 400, 500, 600, 800 and 1000 equivalents (blue bold line) of NaBAr<sub>4</sub> in CHCl<sub>3</sub>/CH<sub>3</sub>CN (v/v, 9:1); (c) Non-linear fitting curve of fluorescence titration.

**3-18. Complexation study if 15 and lithium salt by  $^1\text{H}$  NMR spectra**

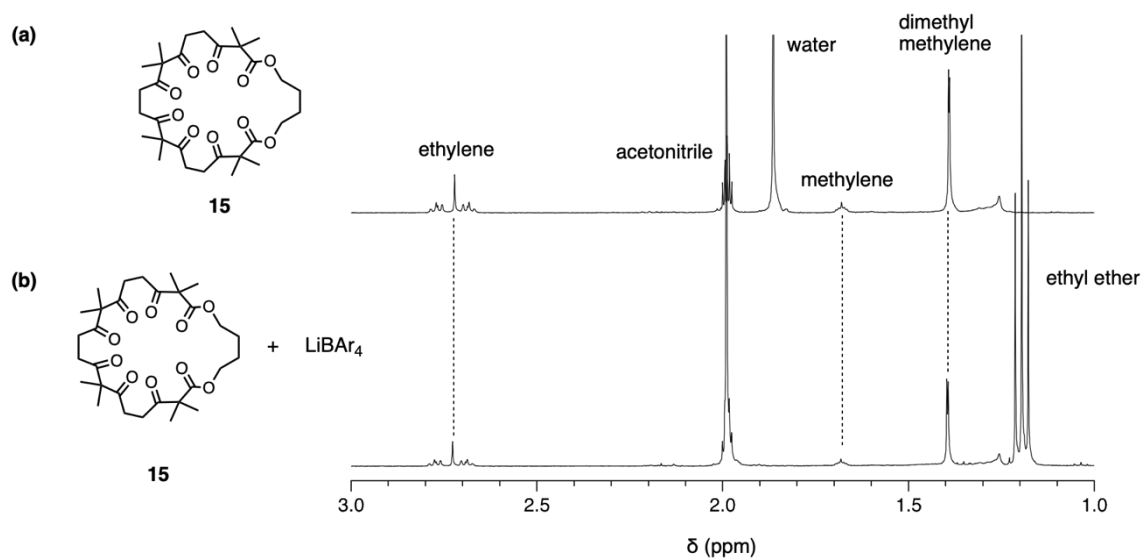


**Figure S18.** (a) Partial  $^1\text{H}$  NMR spectrum of Host **15** (0.5 mM) in  $\text{CDCl}_3/\text{CD}_3\text{CN}$  (v/v, 9:1) at 298 K; (b) Partial  $^1\text{H}$  NMR spectrum of Host **15** in the presence of  $\text{LiBAr}_4$  (5 mM, 10 eq.) in  $\text{CDCl}_3/\text{CD}_3\text{CN}$  (v/v, 9:1) at 298 K. No chemical shift changes of ethylene, methylene, and dimethylmethylenes protons signals indicate no complexation between host **15** and  $\text{LiBAr}_4$ .

**3-19.  $^1\text{H}$  NMR spectroscopic titration of **15** with sodium salt**

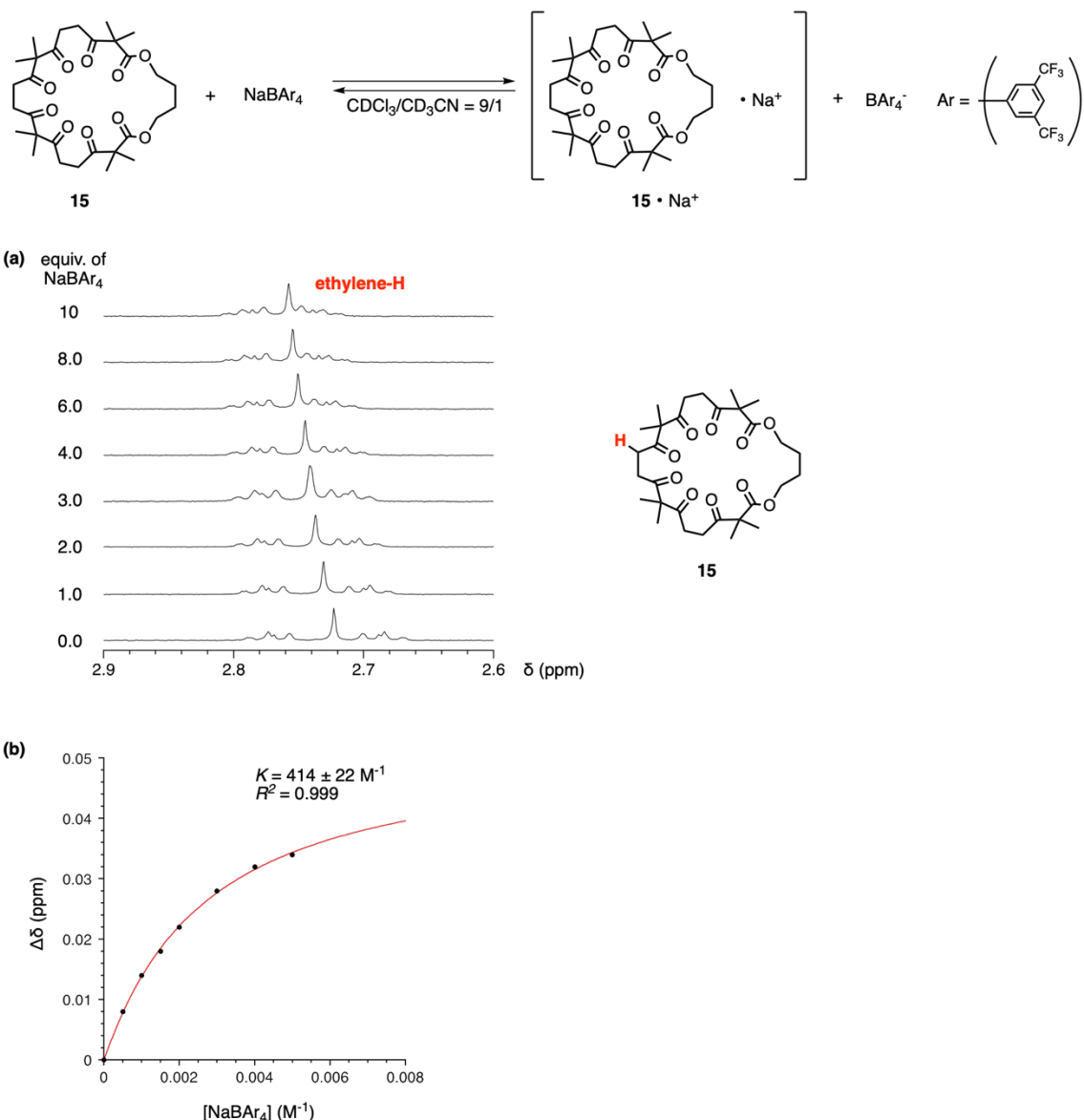


**Figure S19.** (a)  $^1\text{H}$  NMR spectra of host **15** (0.5 mM) with increasing the ratio of NaBAr<sub>4</sub> from 0.0 to 10 eq. in CDCl<sub>3</sub>/CD<sub>3</sub>CN (v/v, 9:1) at 298 K; (b) Non-linear fitting curve of  $^1\text{H}$  NMR titration.

**3-20.  $^1\text{H}$  NMR spectroscopic titration of **15** with potassium salt**

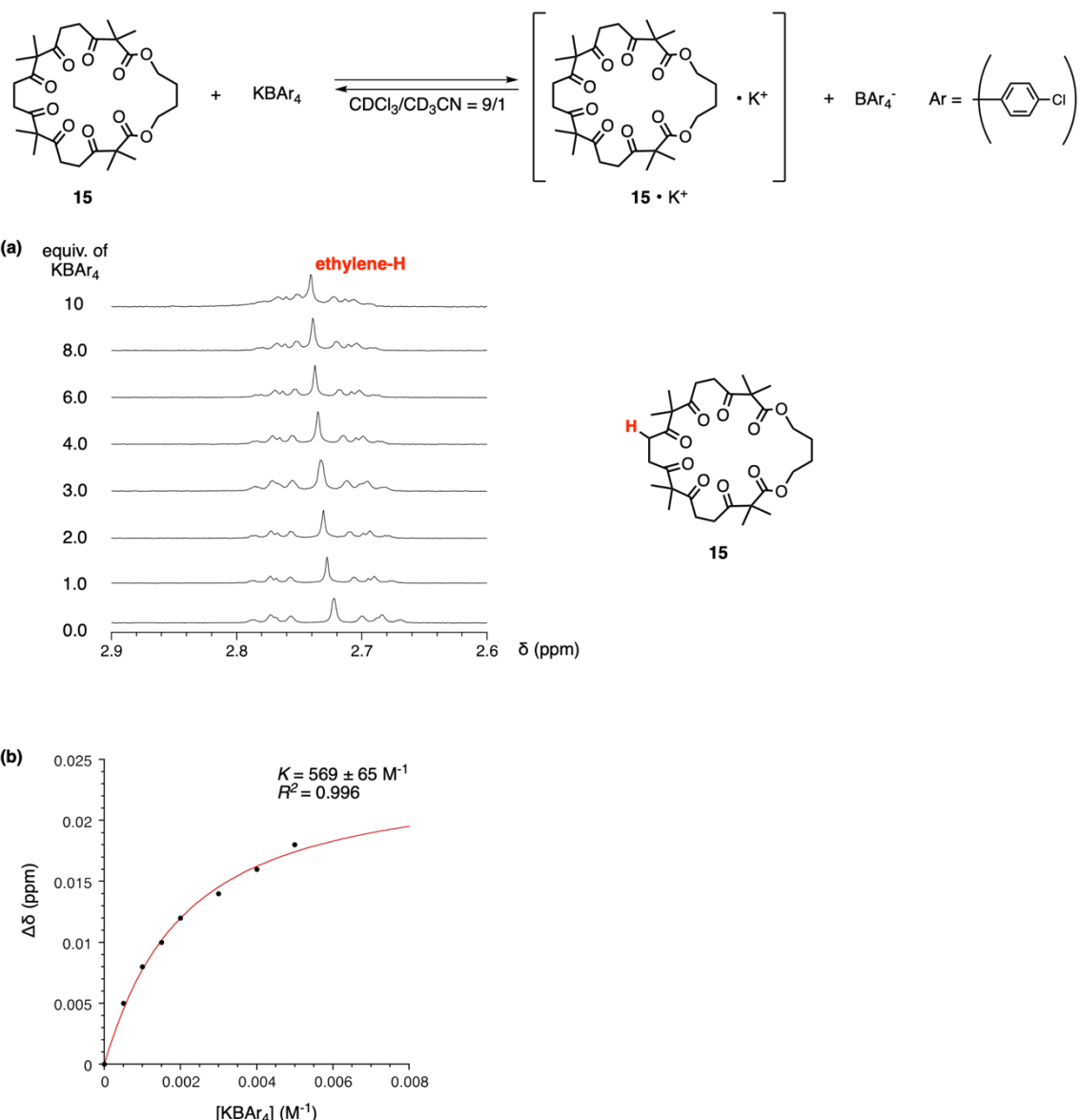


**Figure S20.** (a)  $^1\text{H}$  NMR spectra of host **15** (0.5 mM) with increasing the ratio of  $\text{KBAr}_4$  from 0.0 to 10 eq. in  $\text{CDCl}_3/\text{CD}_3\text{CN}$  (v/v, 9:1) at 298 K; (b) Non-linear fitting curve of  $^1\text{H}$  NMR titration.

## 4. X-ray Crystallographic Analysis

### 4-1. Single crystal X-ray diffraction analysis for **5**

Single crystals of **5** suitable for X-ray diffraction analysis were obtained by vapor diffusion of hexane into a dichloromethane solution of **5**.

$C_{35}H_{50}O_{10}$ ,  $M = 630.75$ , crystal size:  $0.45 \times 0.25 \times 0.10$  mm $^3$ , monoclinic, space group  $P2_1/n$ ,  $a = 24.7386(8)$ ,  $b = 20.8849(4)$ ,  $c = 27.7039(9)$  Å,  $\alpha = \gamma = 90^\circ$ ,  $\beta = 109.539(4)^\circ$ ,  $V = 13489.3(7)$  Å $^3$ ,  $Z = 16$ ,  $T = 123(2)$  K,  $\mu = 0.090$  mm $^{-1}$ ,  $D_{\text{calc}} = 1.242$  g/cm $^3$ ,  $1.840^\circ \leq \theta \leq 26.499^\circ$ , 18985 unique reflections out of 27905 with  $I > 2\sigma(I)$ , GOF = 1.042,  $R_1 = 0.0570$ ,  $wR_2 = 0.1446$ , CCDC: 2141342

Asymmetric unit for the crystal structure of **5** contained two pairs of conformational enantiomers (unit 1 and unit 2, unit 3 and unit 4, see Figure S21).

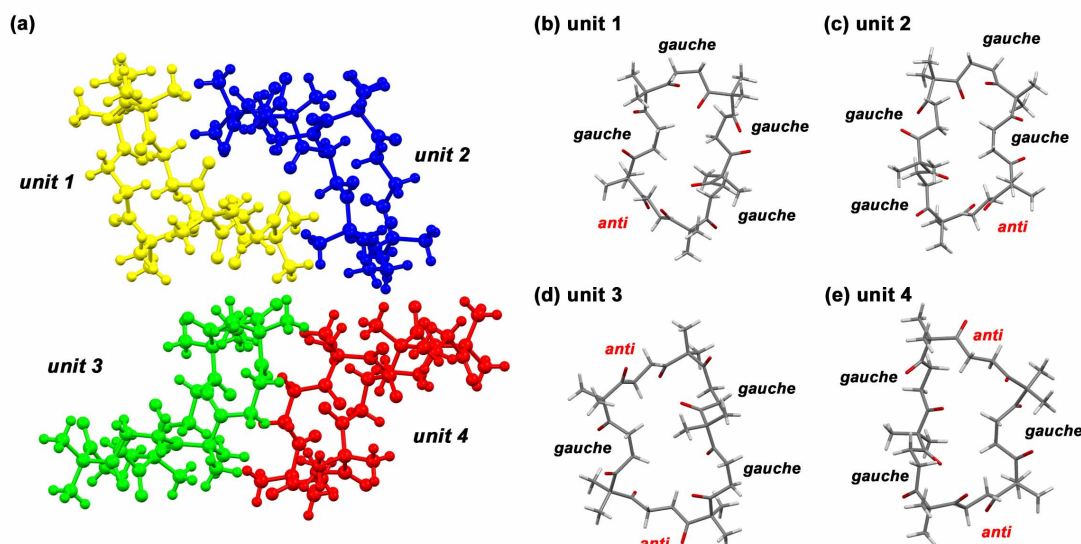


**Figure S21.** (a) Asymmetric unit for the crystal structure of **5** showing four individual units as yellow, blue, light green, and red; (b–e) conformation of **5** at unit 1–4.

#### 4-2. Single crystal X-ray diffraction analysis for **5•K<sup>+</sup>**

Potassium complex of **5** was crystallized by vapor diffusion of chloroform and hexane into a acetonitrile solution containing **5** and KBAr<sub>4</sub> (Ar = 4-chlorophenyl) in a 1:1 molar ratio.

C<sub>35</sub>H<sub>50</sub>O<sub>10</sub>K•C<sub>24</sub>H<sub>16</sub>BCl<sub>4</sub>•(CHCl<sub>3</sub>)<sub>0.176</sub>•(C<sub>2</sub>H<sub>3</sub>N)<sub>2.824</sub>,  $M = 1263.77$ , crystal size: 0.43 × 0.30 × 0.11 mm<sup>3</sup>, triclinic, space group  $P\bar{1}$ ,  $a = 14.3354(3)$ ,  $b = 15.5230(4)$ ,  $c = 16.9525(4)$  Å,  $\alpha = 107.967(2)$ ,  $\beta = 106.917(2)$ ,  $\gamma = 102.643(2)$ °,  $V = 3229.71(14)$  Å<sup>3</sup>,  $Z = 2$ ,  $T = 123(2)$  K,  $\mu = 0.328$  mm<sup>-1</sup>,  $D_{\text{calc}} = 1.300$  g/cm<sup>3</sup>,  $2.194^\circ \leq \theta \leq 26.499^\circ$ , 10282 unique reflections out of 13182 with  $I > 2\sigma(I)$ , GOF = 1.046,  $R_1 = 0.0563$ ,  $wR_2 = 0.1543$ , CCDC: 2141343

#### 4-3. Single crystal X-ray diffraction analysis for **6**

Single crystals of **6** suitable for X-ray diffraction analysis were obtained by vapor diffusion of hexane into a dichloromethane solution of **6**.

C<sub>42</sub>H<sub>60</sub>O<sub>12</sub>•(CH<sub>2</sub>Cl<sub>2</sub>)<sub>2</sub>,  $M = 926.75$ , crystal size: 0.50 × 0.40 × 0.20 mm<sup>3</sup>, monoclinic, space group  $P2_1/n$ ,  $a = 21.2562(7)$ ,  $b = 11.1760(3)$ ,  $c = 22.0433(7)$  Å,  $\alpha = \gamma = 90$ ,  $\beta = 113.739(4)$ °,  $V = 4793.5(3)$  Å<sup>3</sup>,  $Z = 4$ ,  $T = 123(2)$  K,  $\mu = 0.304$  mm<sup>-1</sup>,  $D_{\text{calc}} = 1.284$  g/cm<sup>3</sup>,  $2.019^\circ \leq \theta \leq 26.999^\circ$ , 8860 unique reflections out of 10420 with  $I > 2\sigma(I)$ , GOF = 1.018,  $R_1 = 0.0474$ ,  $wR_2 = 0.1294$ , CCDC: 2141344

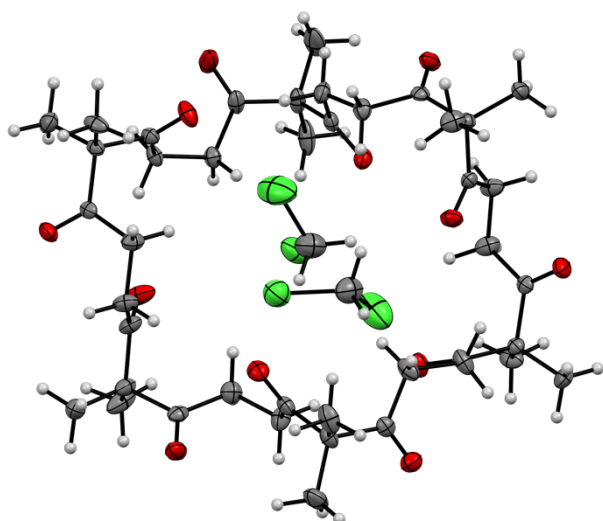


**Figure S22.** ORTEP drawing of the asymmetric unit for crystal structure of **6•(CH<sub>2</sub>Cl<sub>2</sub>)<sub>2</sub>** at the 50% probability levels (C: gray, H: white, O: red, Cl: green).

## 5. Theoretical Calculations

### Theoretical model of **6•K<sup>+</sup>**

To theoretically investigate **K<sup>+</sup>** binding form by **6**, we located **K<sup>+</sup>** inside **6** ring obtained from the single crystal X-ray analysis. First, the prepared initial structure of **6•K<sup>+</sup>** was optimized by the self-consistent-charge density-functional tight binding (DFTB) method with the third-order expansion as implemented in the DFTB+ package version 21.1.<sup>11</sup> The 3ob parameter set<sup>12, 13</sup> with Hubbard parameters -0.1492 for C, -0.1857 for H, -0.1575 for O, and -0.0339 for K were employed. Grimme's D3 type dispersion<sup>14, 15</sup> was included in all DFTB calculations. After the optimization, we employed DFTB with molecular dynamics simulation (DFTB-MD) for 200 ps with 0.2 fs time interval with an NVT ensemble at 300 K and the Nose–Hoover chain thermostat<sup>16, 17</sup>. Structures every 1 ps from the trajectory of DFTB-MD, i.e. 200 structures, were optimized by DFTB again. The most stable structure among 200 optimized structures was further optimized at M06/6-311+G(d) level of theory<sup>18</sup> with the polarizable continuum model (IEFPCM)<sup>19</sup> for solvation effect of CHCl<sub>3</sub> solvent using Gaussian 16 Rev. C01.<sup>20</sup> The final optimized structure is shown in **Figure S23**.

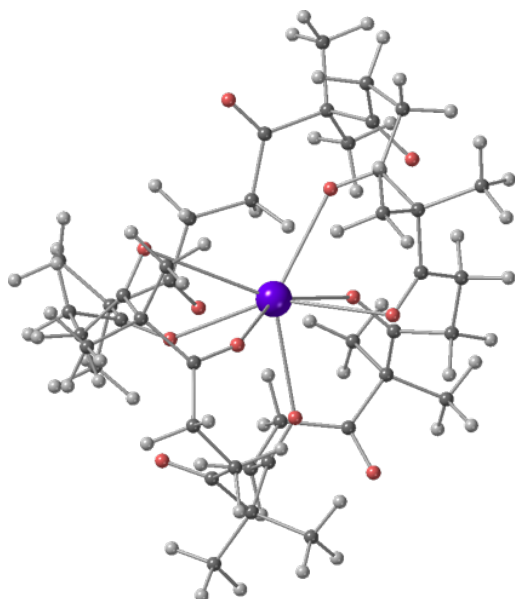


**Figure S23.** Optimized structure of **6•K<sup>+</sup>**. Gray, red, white, and purple spheres indicate carbon, oxygen, hydrogen, and potassium atoms, respectively.

### Theoretical model of **13** and **13•Na<sup>+</sup>**

Similarly to **6•K<sup>+</sup>**, we theoretically investigated the stable structure of **13•Na<sup>+</sup>**. Prior to the calculations of **13•Na<sup>+</sup>**, we optimized **13** by DFTB followed by DFTB-MD, re-optimization by DFTB, and optimization at M06/6-311+G(d) level of theory with IEFPCM (solvent = CHCl<sub>3</sub>) as well. After we obtain the most stable structure among 200 structures, we located Na<sup>+</sup> inside the pseud-ring of **13**, and the same procedures for **6•K<sup>+</sup>** were conducted. Hubbard parameters of -0.0454 for Na was employed. The final optimized structures of **13** and **13•Na<sup>+</sup>** are shown in **Figure S24**.

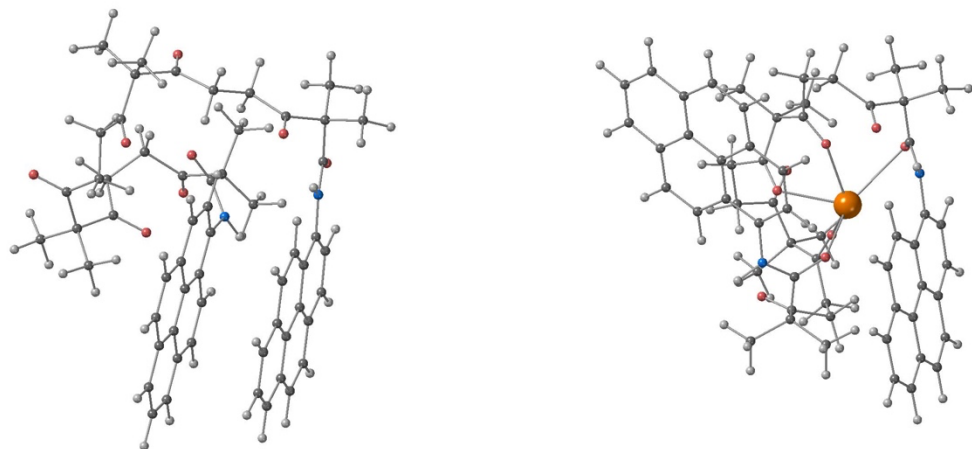
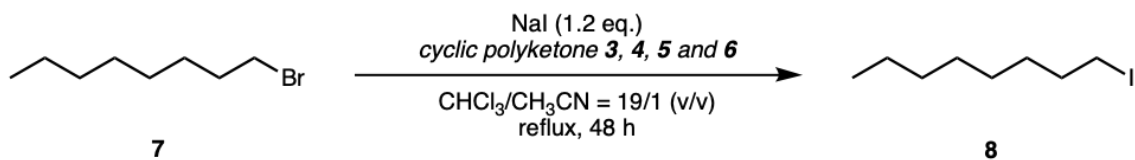


**Figure S24.** Optimized structure of **13** (left) and **13•Na<sup>+</sup>** (right). Gray, red, blue, white, and orange spheres indicate carbon, oxygen, nitrogen, hydrogen, and sodium atoms, respectively.

## 6. Finkelstein Reaction Catalyzed by Cyclic polyketone

### Detailed Procedure



To a solution of 1-bromooctane **7** (100 mg, 0.518 mmol) and 1,3,5-trimethoxybenzene (internal standard, 87.1 mg, 0.518 mmol) in chloroform/acetonitrile=19/1 (v/v) (500  $\mu$ L), were added sodium iodide (93.1 mg, 0.621 mmol) and cyclic polyketone **3**, **4**, **5** or **6** (0.0518 mmol, 10 mol%) at room temperature, and the rection mixture was stirred at reflux for 48 h. The yield of 1-iodooctane **8** was determined by  $^1\text{H}$  NMR spectra compared with the internal standard. The catalyst **6** of 5 mol% and 20 mol% (entry 6 and 7) were performed under the same condition.

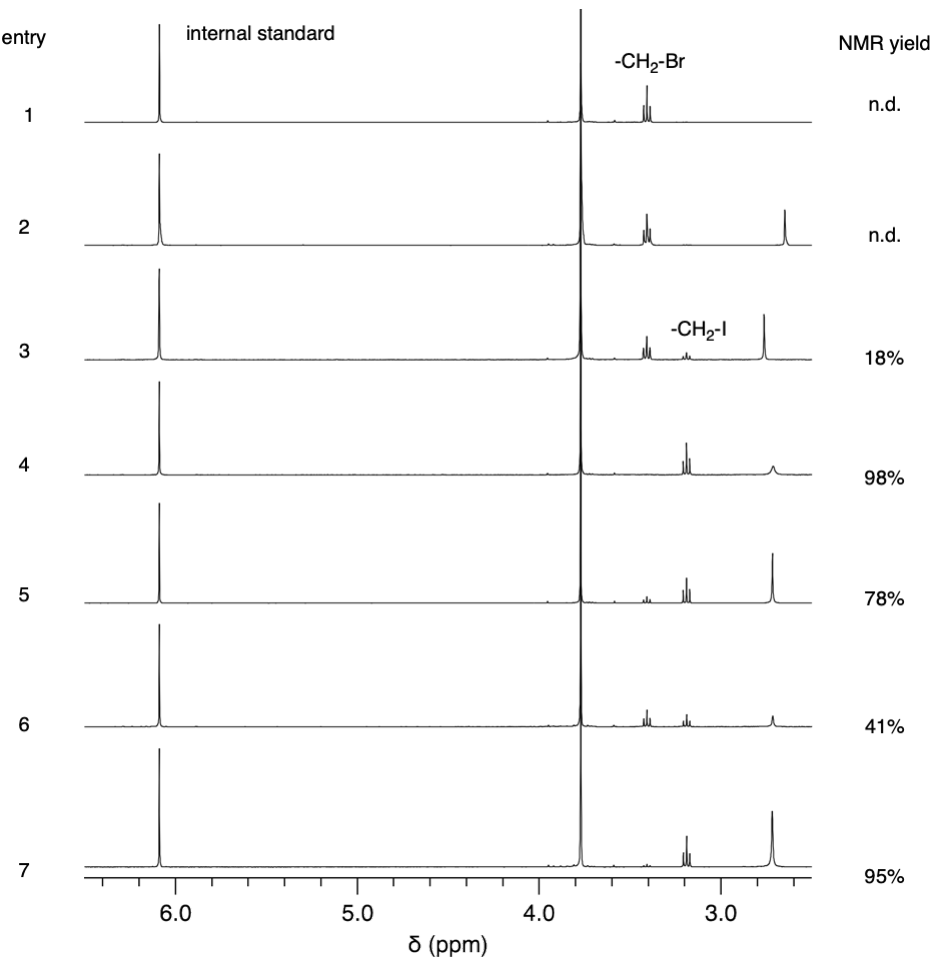


**Figure S25.**  $^1\text{H}$  NMR spectra of the reaction mixture after 48 h (400 MHz, 298 K).

## 7. NMR spectra

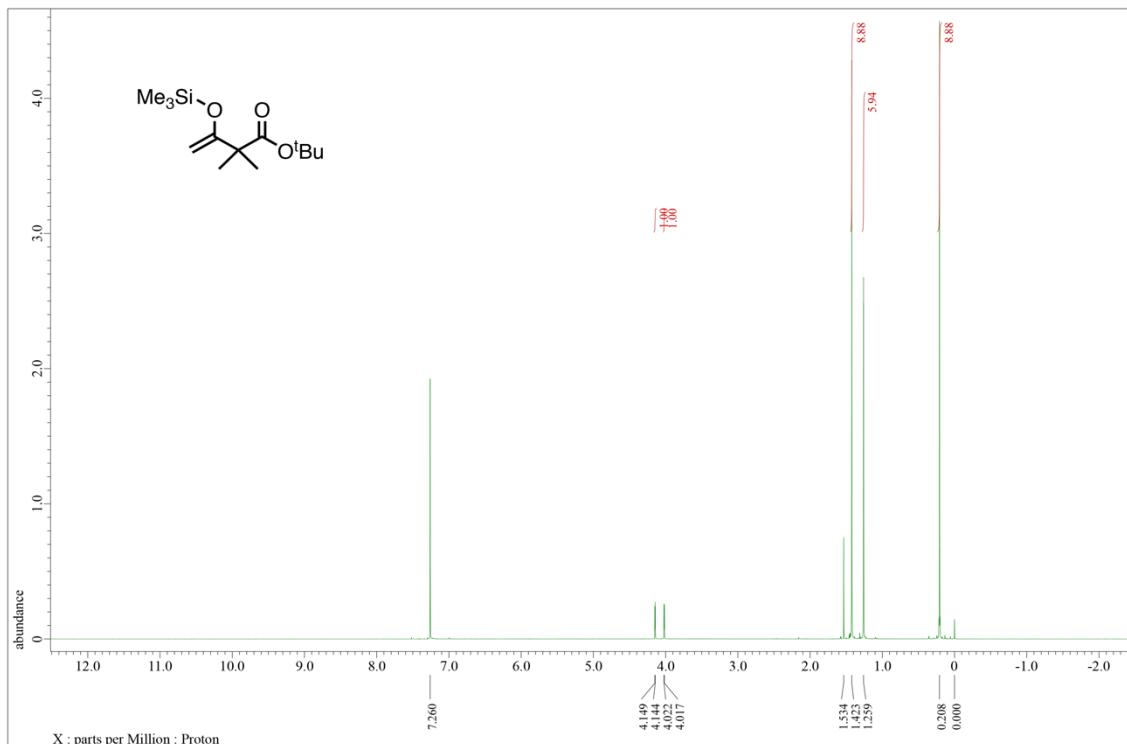


**Figure S26.**  $^1\text{H}$  NMR spectrum of compound **10** in  $\text{CDCl}_3$  (298 K, 400 MHz).

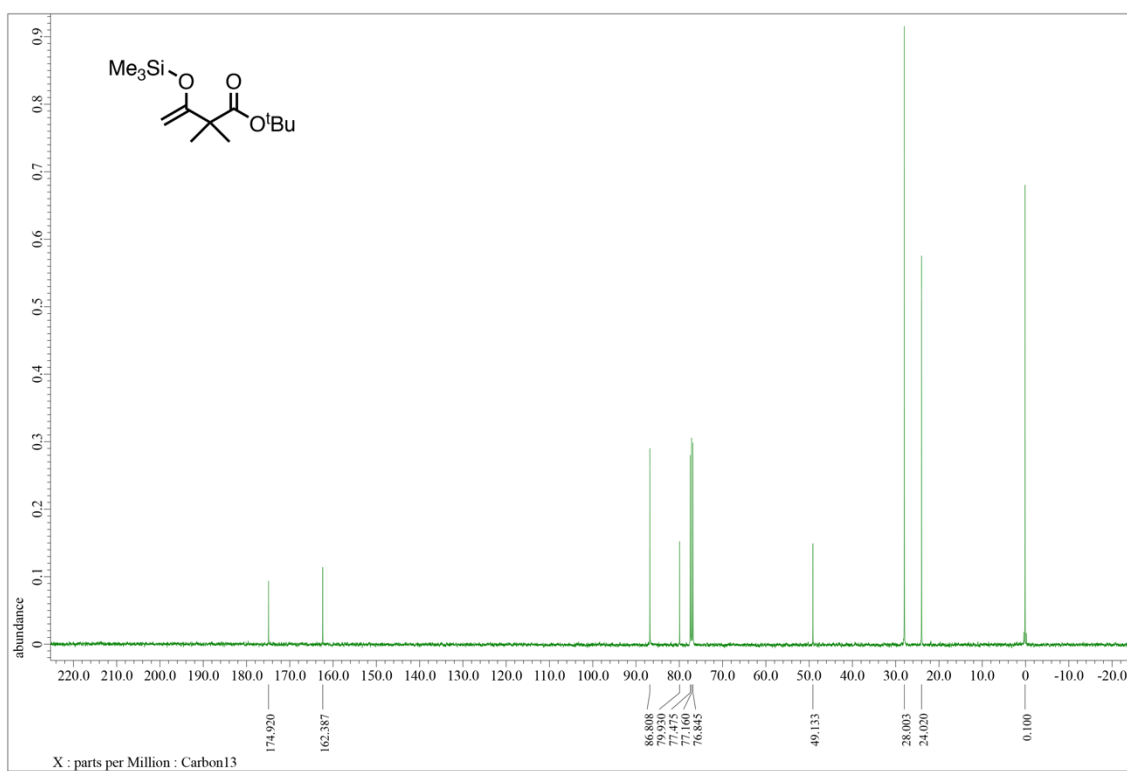


**Figure S27.**  $^{13}\text{C}\{^1\text{H}\}$  NMR spectrum of compound **10** in  $\text{CDCl}_3$  (298 K, 100 MHz).

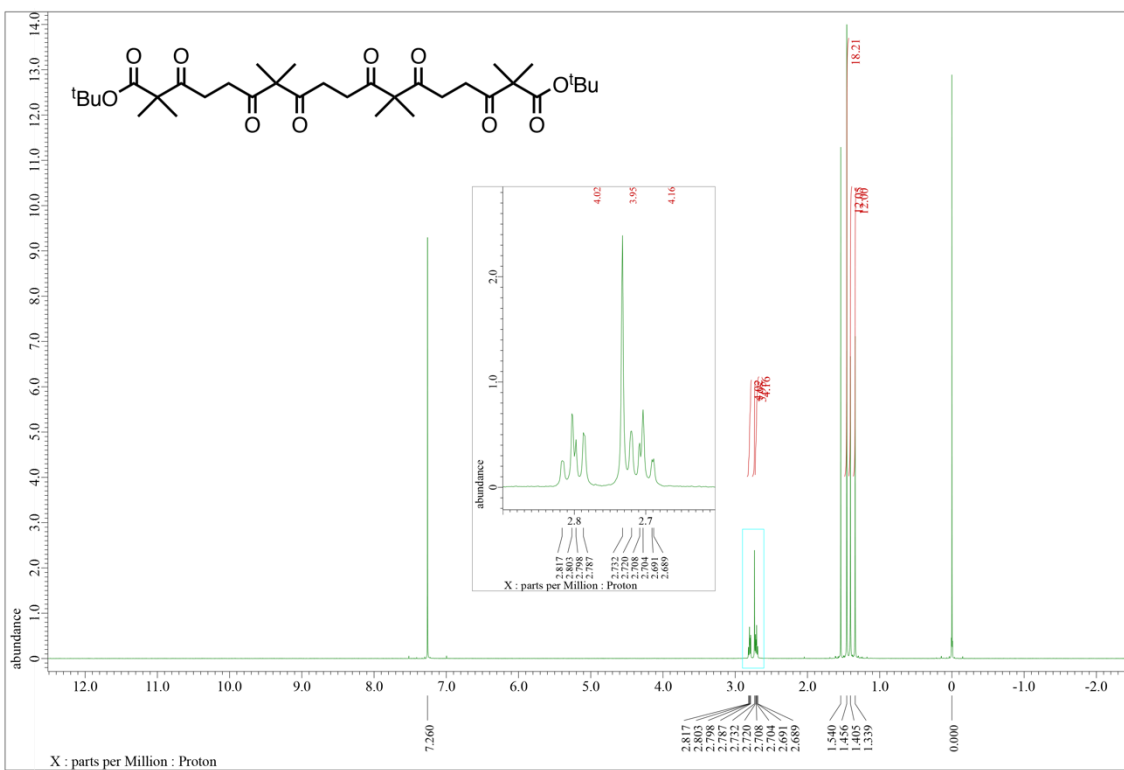


**Figure S28.**  $^1\text{H}$  NMR spectrum of compound **11** in  $\text{CDCl}_3$  (298 K, 400 MHz).

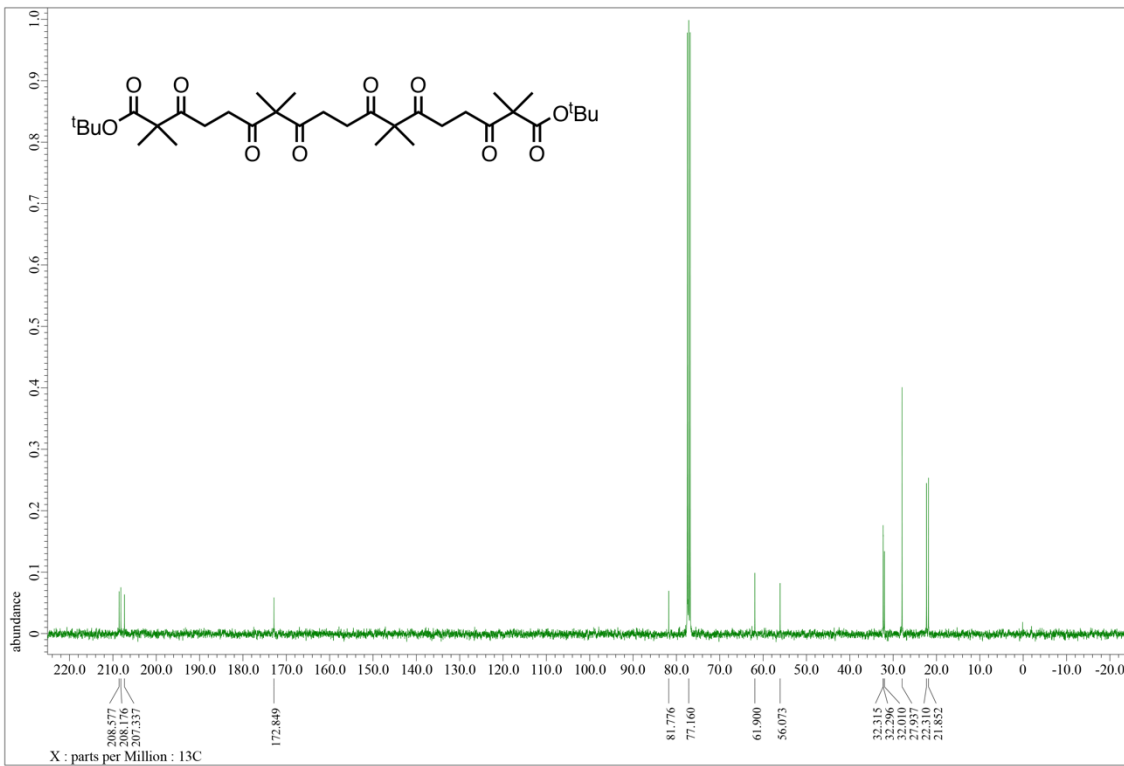


**Figure S29.**  $^{13}\text{C}\{^1\text{H}\}$  NMR spectrum of compound **11** in  $\text{CDCl}_3$  (298 K, 100 MHz).

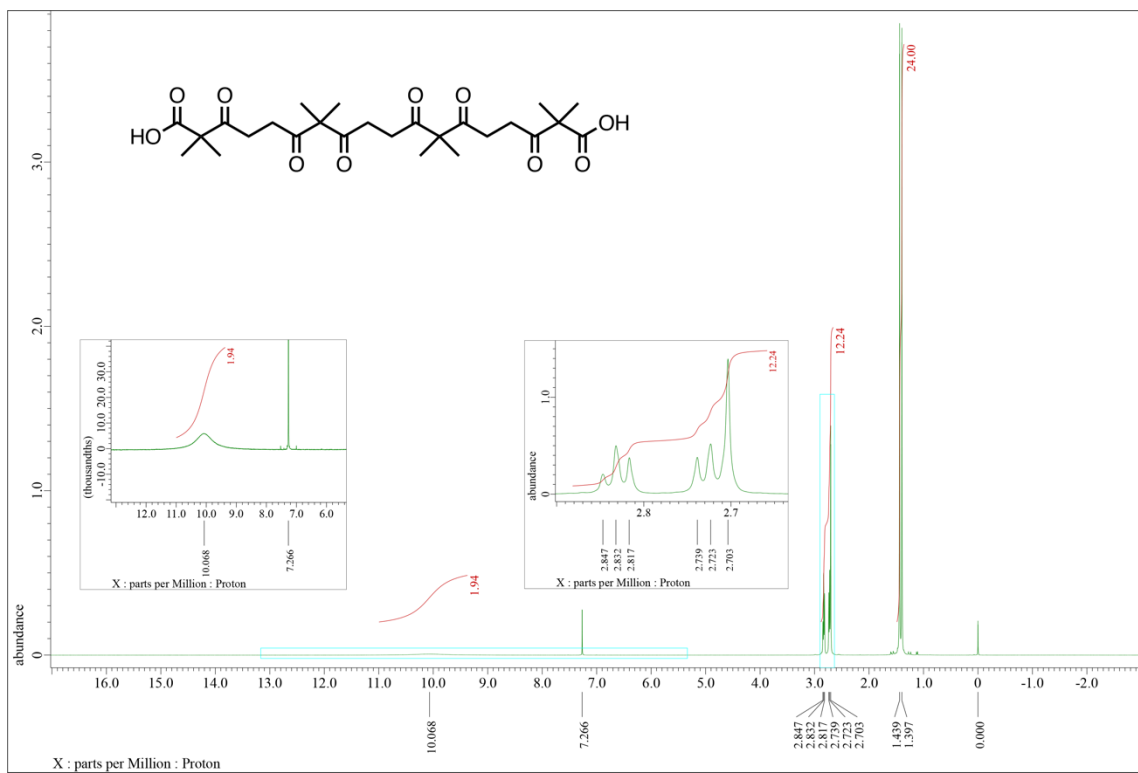


**Figure S30.**  $^1\text{H}$  NMR spectrum of compound **12** in  $\text{CDCl}_3$  (298 K, 400 MHz).

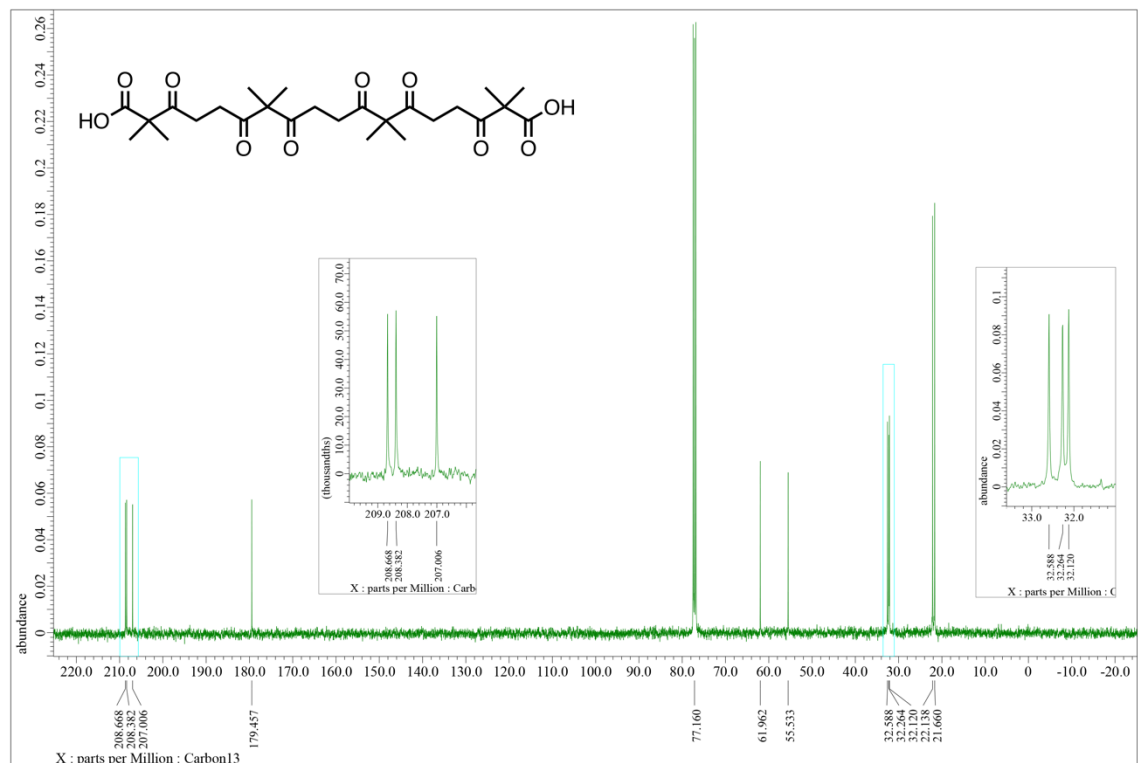


**Figure S31.**  $^{13}\text{C}\{^1\text{H}\}$  NMR spectrum of compound **12** in  $\text{CDCl}_3$  (298 K, 100 MHz).

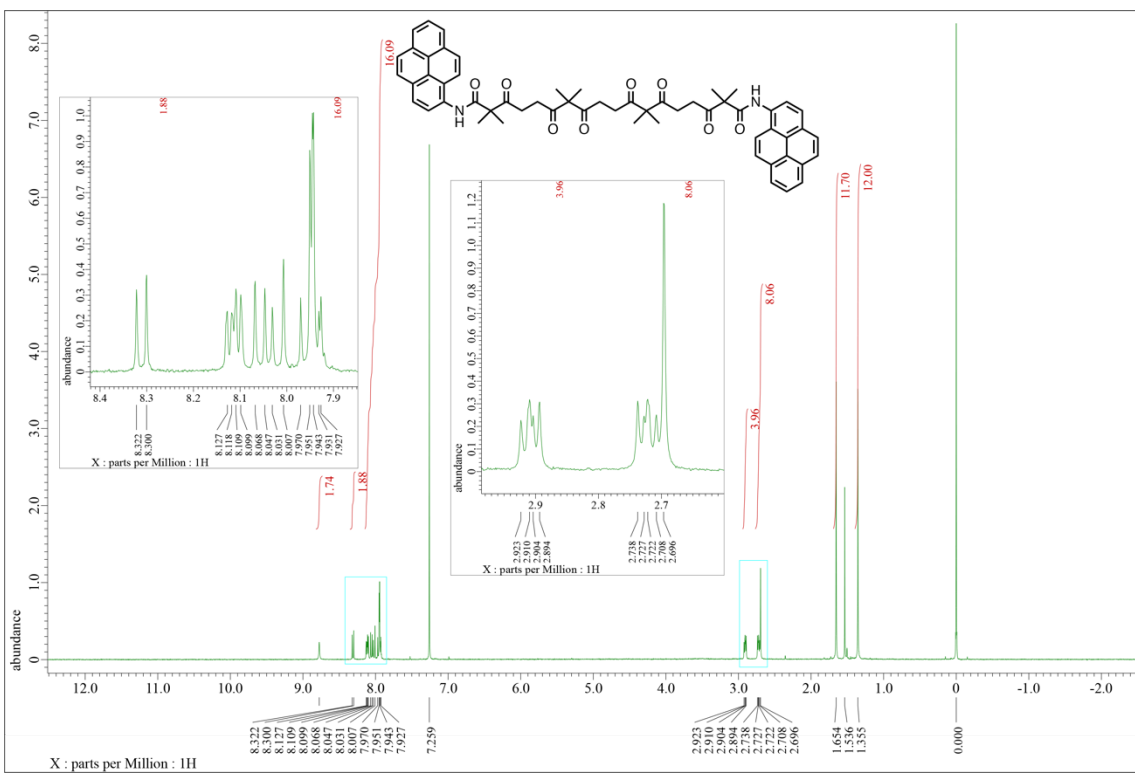


**Figure S32.**  $^1\text{H}$  NMR spectrum of compound **13** in  $\text{CDCl}_3$  (298 K, 400 MHz).

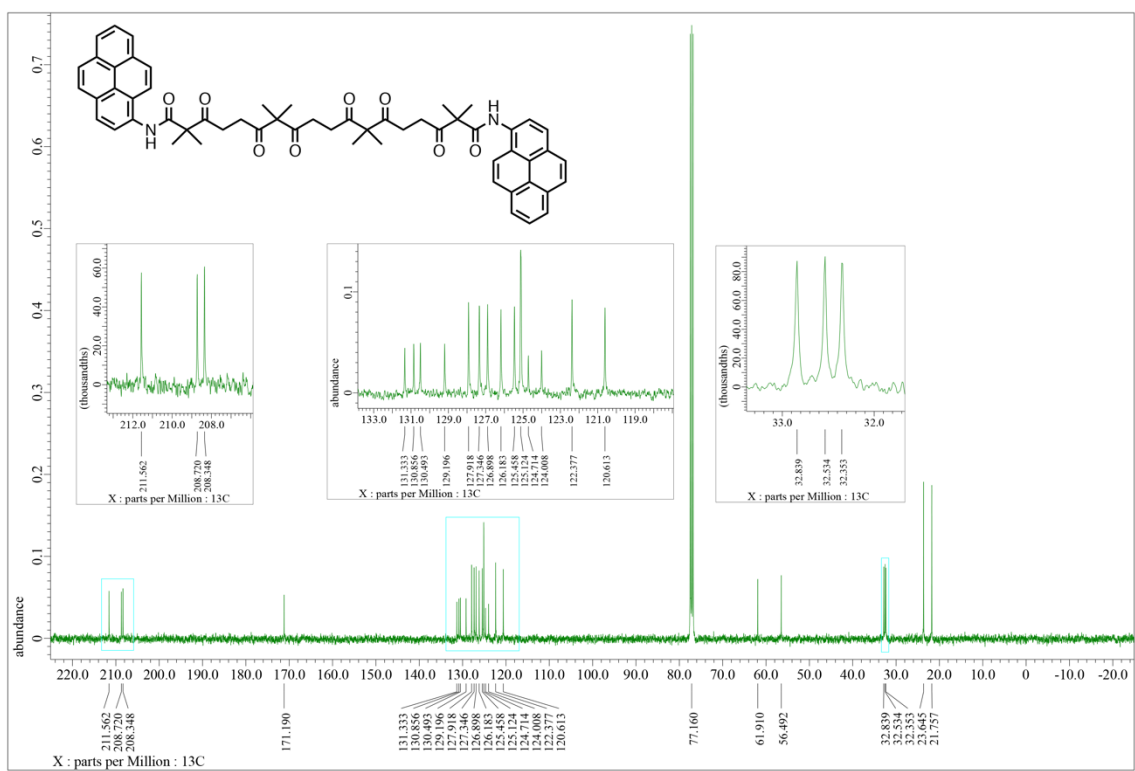


**Figure S33.**  $^{13}\text{C}\{\text{H}\}$  NMR spectrum of compound **13** in  $\text{CDCl}_3$  (298 K, 100 MHz).

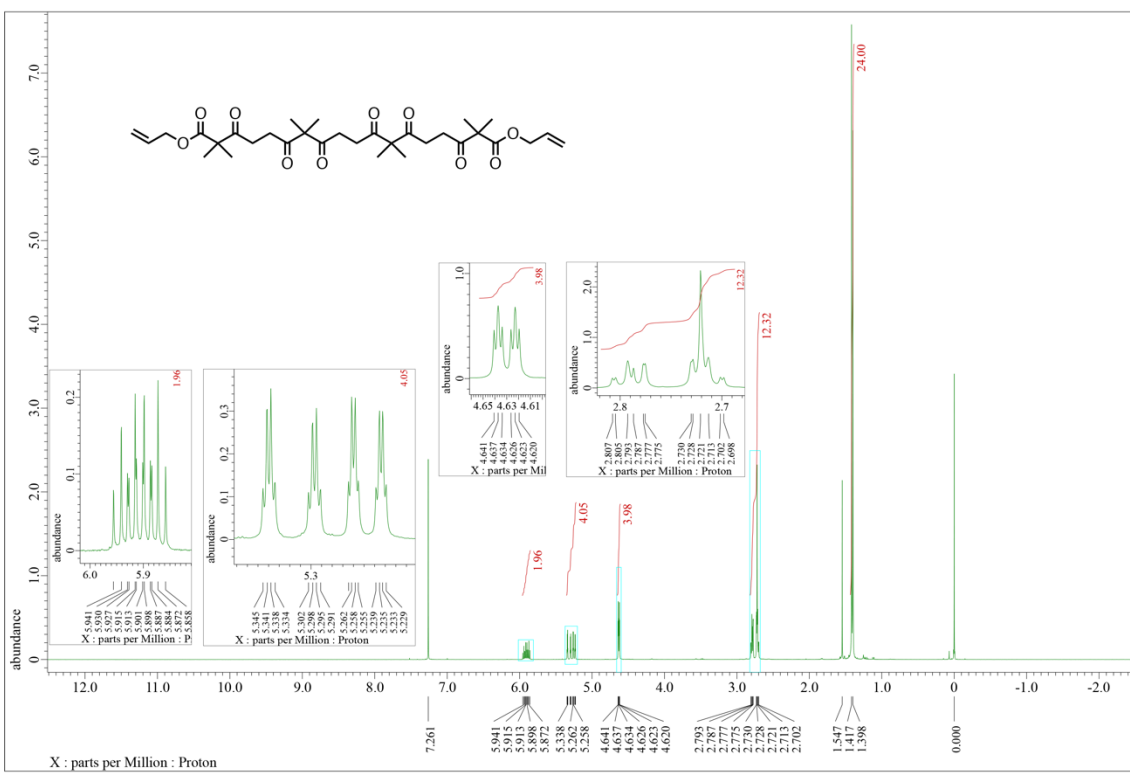


**Figure S34.** <sup>1</sup>H NMR spectrum of compound 14 in CDCl<sub>3</sub> (298 K, 400 MHz).

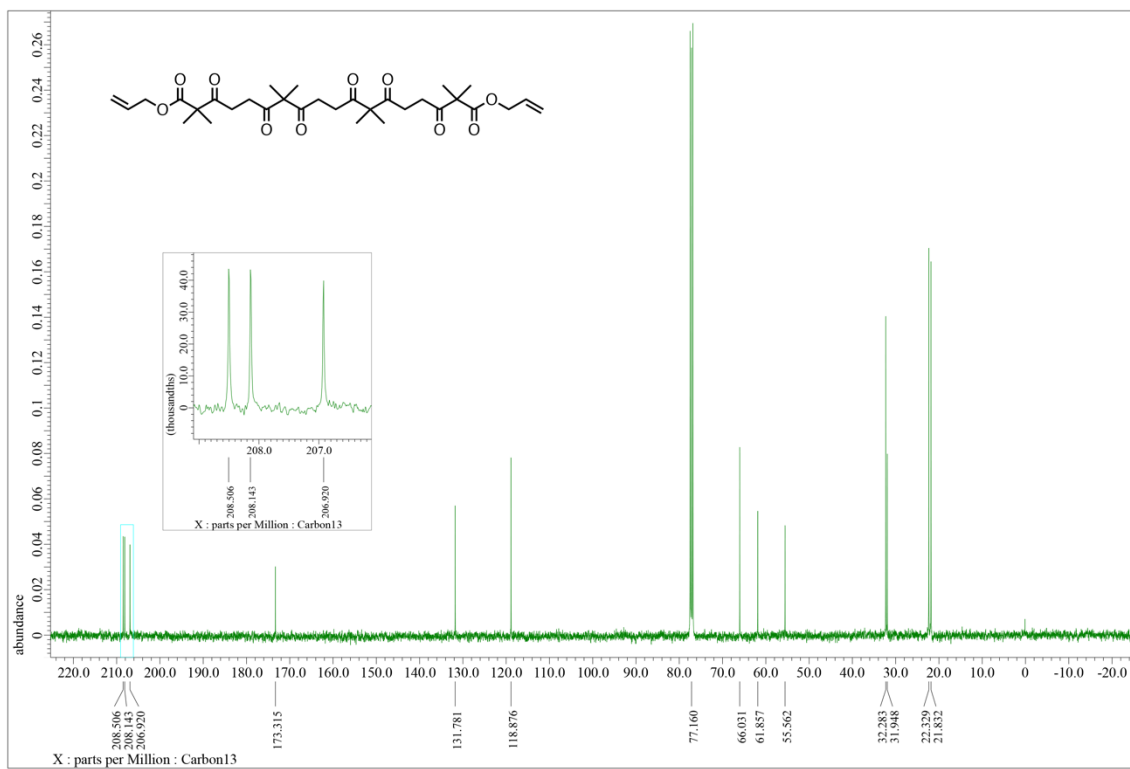


**Figure S35.** <sup>13</sup>C{<sup>1</sup>H} NMR spectrum of compound 14 in CDCl<sub>3</sub> (298 K, 100 MHz).

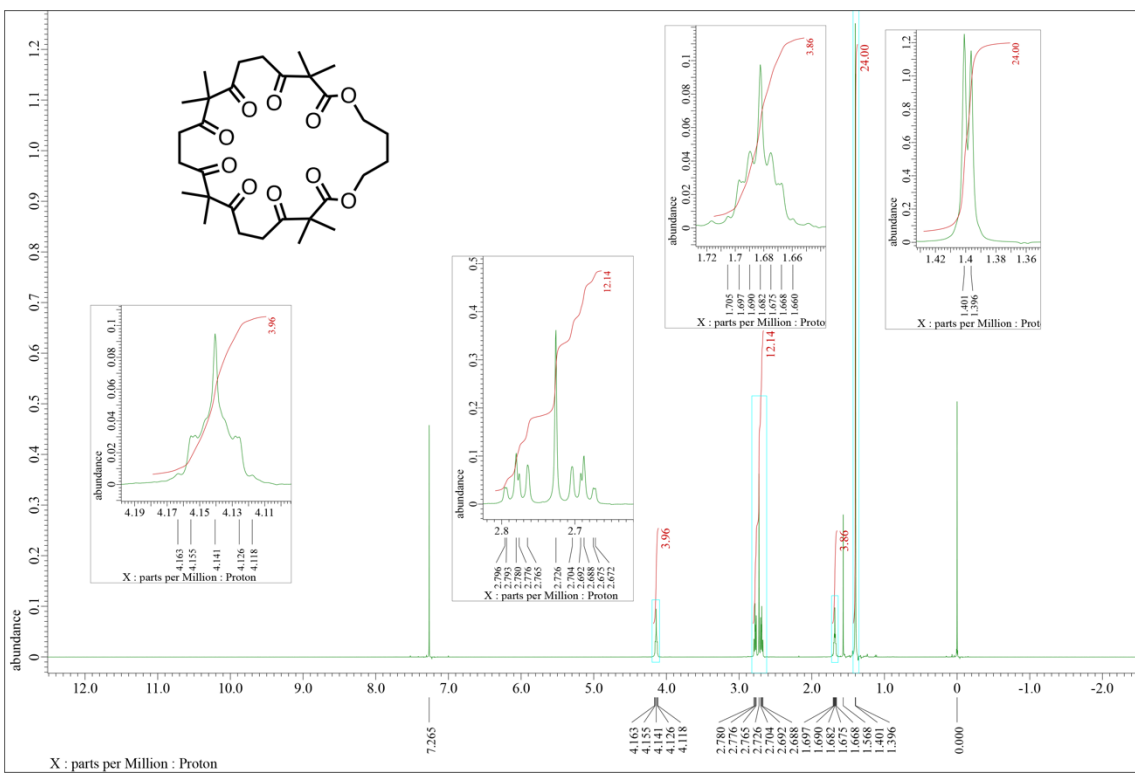


**Figure S36.**  $^1\text{H}$  NMR spectrum of compound **15** in  $\text{CDCl}_3$  (298 K, 400 MHz).

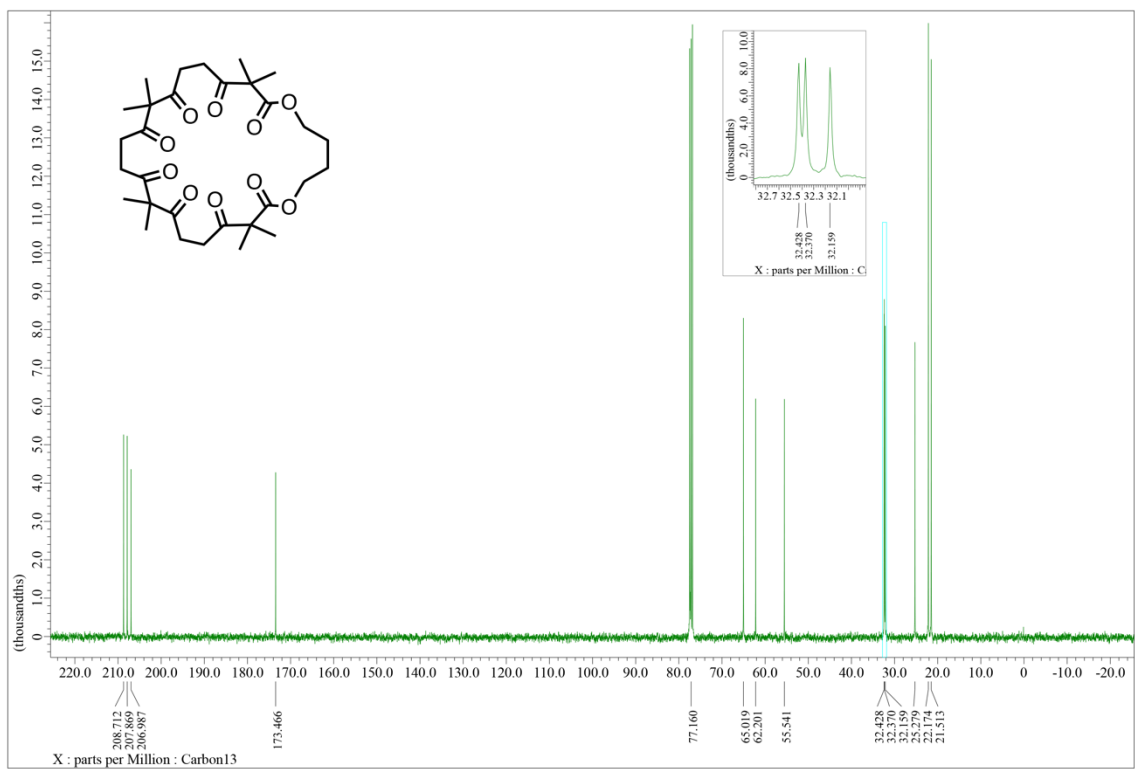


**Figure S37.**  $^{13}\text{C}\{^1\text{H}\}$  NMR spectrum of compound **15** in  $\text{CDCl}_3$  (298 K, 100 MHz).

## 8. Cartesian Coordinates of Optimized Structure

Cartesian Coordinates of the optimized **6•K<sup>+</sup>**

C	3.65059700	-2.52642600	2.18470500	H	2.67660500	1.34291500	-2.78649900
C	3.54910200	-2.95397600	-0.37004700	H	2.61224700	3.09213800	-2.80526400
C	2.94074100	-2.98144300	3.46164600	H	3.81037800	1.72012500	2.24229300
H	4.35222100	-3.69966700	-0.30887900	H	5.53122400	1.86805800	1.97264700
H	4.05992600	-1.98670100	-0.48623000	H	5.70478000	-0.67021200	1.81462500
H	3.27732600	-3.53465500	-2.42894800	H	5.12330000	-0.13770100	3.37697700
H	4.71899200	3.62228900	-2.17202200	H	2.05625900	-4.16054300	-1.35853400
H	3.29056600	3.64348400	1.26826900	H	-0.86153600	-2.55725600	-1.14794200
H	2.91261600	-4.07517900	3.50683000	H	-1.66981400	-3.25948700	-2.50445100
H	1.91604600	-2.60949800	3.50451900	H	-2.41740900	-0.55295300	-1.24281500
H	3.48149200	-2.62145800	4.34452800	H	-3.01210800	-1.08149800	-2.78005400
H	0.25543800	-4.39685800	-2.88671200	H	-4.19867300	-2.48682100	1.55495500
O	2.52427300	-0.44227700	2.15517100	H	-5.80556600	-1.93510600	1.95901300
C	-2.84228600	-0.33477400	2.69026000	H	-4.89623000	0.07201000	3.12635000
C	-2.22227700	0.71779700	3.62047800	H	-4.26404800	-1.39274600	3.83148800
C	-1.60138400	1.77574700	2.69135600	H	-4.05410200	1.86098800	4.08224100
C	-2.56612200	2.68600800	1.97895300	H	-2.69515100	2.14186900	5.17476700
C	-1.99852200	3.45569100	0.80290800	H	-3.61380400	0.64348700	5.28646600
C	-1.74614400	2.60192000	-0.40912700	H	-0.63246600	0.71552400	5.09024200
C	-1.54989500	3.28001100	-1.77848200	H	-0.38055500	-0.45767200	3.79064100
C	-0.01717500	3.34792400	-1.95579000	H	-1.58625900	-0.77777600	5.05097200
C	0.68535800	2.13929700	-2.51666000	H	-1.87162300	1.37815200	-2.84983600
C	2.18099100	2.20890000	-2.32031300	H	-2.02178400	2.83647000	-3.84668800
C	2.56253600	2.19291000	-0.87078500	H	-3.29806800	2.41463500	-2.70276600
C	4.01014100	2.49330200	-0.45449800	H	-1.64786300	5.37176900	-1.12775500
C	4.43778900	1.21088000	0.27577900	H	-3.19989000	4.68226400	-1.66047000
C	4.66339600	1.22701700	1.76264700	H	-1.95721400	5.10814000	-2.84009100
C	4.86630200	-0.17176400	2.30679600	H	5.00504800	1.87100200	-2.30611800
C	3.60484100	-0.98893300	2.19170800	H	5.99168300	2.85918400	-1.22510300
C	2.82547600	-2.94106800	0.94979800	H	3.60870000	4.59448800	-0.18301200
C	2.66663700	-3.26750000	-1.55559600	H	4.96540300	4.00518800	0.78252900
C	1.73028500	-2.16708700	-1.95467600	H	5.60660000	-2.83328800	3.06344700
C	0.93032200	-2.32895100	-3.24449100	H	5.65462200	-2.77695900	1.29769800
C	-0.42804900	-1.63730400	-3.04655500	H	5.01548200	-4.20132800	2.12601600
C	-1.38469800	-2.28684600	-2.07789800	H	0.04156400	-3.81180200	-4.54248100
C	-2.62833000	-1.46394800	-1.82588800	H	1.64588900	-4.25271600	-3.97131400
C	-3.72000200	-2.23458100	-1.13802700	H	2.73265800	-2.03839600	-4.42800500
C	-5.04217700	-1.48712300	-0.85008600	H	1.84383200	-0.53558500	-4.08826400
C	-4.85319400	-0.74747900	0.48289200	H	1.22623100	-1.68013700	-5.28708900
C	-4.78860900	-1.58216400	1.73999200	H	-6.34797000	-0.02129700	-1.74174700
C	-4.25580500	-0.78921000	2.91076200	H	-5.44693900	-0.98428300	-2.91939900
C	-3.21022300	1.37774000	4.58160300	H	-4.64378200	0.32319400	-2.01990000
C	-1.13775400	0.00521500	4.42827100	H	-7.10329500	-2.00077700	-0.41316300
C	-2.21207200	2.41540600	-2.85337200	H	-5.95658600	-3.29571700	-0.00289200
C	-2.11930300	4.69201900	-1.83998800	H	-6.36170400	-2.97774300	-1.68780000
C	4.97699300	2.71627700	-1.61445600	O	-2.15798000	-0.81804500	1.81238300
C	3.96550300	3.74825800	0.41576200	O	-0.40449000	1.86643600	2.55031800
C	5.06043500	-3.10682700	2.15415400	O	-1.65336500	1.39682600	-0.30949300
C	0.70544100	-3.78079500	-3.67097500	O	0.59038100	4.34271800	-1.63764500
C	1.73512500	-1.59819800	-4.32162600	O	1.75342500	1.92894200	-0.00700800
C	-5.37689300	-0.48358100	-1.94724000	O	4.57378300	0.19497300	-0.37110800
C	-6.17812300	-2.50243300	-0.71842400	O	1.64931700	-3.20358700	1.03868400
H	-2.93445100	3.40188300	2.72805300	O	1.62769700	-1.13729700	-1.31760200
H	-3.45038300	2.10913500	1.67103400	O	-0.72701500	-0.65032200	-3.67420700
H	-2.66535400	4.28443800	0.54910600	O	-3.57915200	-3.38979800	-0.81338000
H	-1.03537100	3.92766700	1.05770100	O	-4.77784000	0.45884800	0.52474100
H	0.43920300	2.07216300	-3.58587000	K	0.29692500	-0.17593900	0.77819000
H	0.26597700	1.22522600	-2.08052700				

## Cartesian Coordinates of the optimized **13**

N	0.41877100	-0.44338900	-1.34997300	H	1.74862500	2.12351100	0.36726200
C	1.76091200	-0.33058500	-1.55713600	C	3.51980900	1.53636200	2.59176600
C	-0.25131700	0.02543400	-0.19986600	H	4.15862300	1.86163300	0.57674500
H	-0.15577800	-0.65905300	-2.15260200	H	4.28948600	3.25177700	1.63121600
C	2.25753500	-0.58734100	-2.98867000	C	4.73665700	0.65289100	2.93036300
O	2.53812800	-0.04001500	-0.66010600	O	2.53016200	1.52674900	3.28415000
C	-1.43923200	0.76578600	-0.33964400	C	4.67344200	-0.56098900	1.98173500
C	0.26513800	-0.24284600	1.06249800	C	6.04162200	1.41242100	2.71449600
C	2.77555400	0.71933100	-3.62720600	C	4.64951300	0.19399600	4.38439300
C	1.21804200	-1.21037200	-3.90663700	C	3.61027000	-1.58832400	2.27073500
C	3.47552100	-1.52330600	-2.90097900	O	5.44144400	-0.67540100	1.05693600
C	-2.08582500	1.23491100	0.83770400	H	6.20309400	1.69964700	1.67405200
C	-2.02940700	1.07408900	-1.60751000	H	6.88765400	0.78363300	3.01165300
C	-0.34613400	0.24159900	2.20178100	H	6.06411600	2.31588500	3.33411300
H	1.16218700	-0.84399300	1.13743300	H	3.69415000	-0.27482800	4.62605200
C	3.71120900	1.61739400	-2.84432300	H	5.45601000	-0.51280500	4.61082000
O	2.53652500	0.96683800	-4.78573300	H	4.76602100	1.05590500	5.04995900
H	1.66827100	-1.43619200	-4.87647500	C	3.45105600	-2.59823400	1.15928600
H	0.37781600	-0.53391700	-4.11103000	H	3.86908700	-2.09389700	3.21193400
H	0.84649000	-2.14883000	-3.48427100	H	2.66585100	-1.07641900	2.49875000
H	4.23173400	-1.15398200	-2.20287700	C	2.28958200	-3.52811700	1.35169300
H	3.14660600	-2.51455500	-2.56833900	H	3.30860400	-2.08330800	0.19370000
H	3.93468900	-1.63761800	-3.88927800	H	4.37270000	-3.17517100	1.02120100
C	-1.52263400	0.98611900	2.11713000	C	2.06006700	-4.62417000	0.29945600
C	-3.29718800	1.97324100	0.73831900	O	1.50259100	-3.39004100	2.26611400
C	-3.19133300	1.76314200	-1.69680300	C	1.02162800	-4.08653000	-0.71879000
H	-1.53064800	0.77165100	-2.52553900	C	3.32805000	-5.01052100	-0.44747600
H	0.08990600	0.03140900	3.17759300	C	1.48238800	-5.87473700	0.97283500
C	3.18388600	3.04526100	-2.74369900	N	-0.15187900	-3.69077300	-0.14733700
H	4.65814700	1.63158200	-3.39842700	O	1.25773000	-4.06547200	-1.91058300
H	3.91830200	1.21705200	-1.84991200	H	3.11001900	-5.81096400	-1.15993200
C	-2.19307700	1.47847300	3.28061700	H	4.08196000	-5.38502200	0.25378600
C	-3.87161100	2.23468300	-0.53203900	H	3.76212700	-4.18336000	-1.01455800
C	-3.94219400	2.44974000	1.91091900	H	0.60830900	-5.66434400	1.59214100
H	-3.62489500	1.98105000	-2.67183000	H	1.19643500	-6.60945800	0.21257900
C	1.80267800	3.10238500	-2.13108700	H	2.24044600	-6.33544200	1.61585900
H	3.09882400	3.48815300	-3.74748000	C	-1.30926100	-3.17777100	-0.75764100
H	3.89415000	3.67398800	-2.19505600	H	-0.15173500	-3.70652300	0.86541700
C	-3.34991900	2.17560800	3.18407400	C	-2.31399300	-2.62271600	0.06742100
H	-1.74759300	1.27496500	4.25344000	C	-1.48068000	-3.20855800	-2.14150200
C	-5.07008000	2.94852800	-0.60866000	C	-3.46514400	-2.05574500	-0.54711600
C	-5.13525300	3.16608500	1.78780200	C	-2.23126600	-2.58548000	1.49830300
C	1.48645300	4.26849400	-1.19420600	C	-2.60652700	-2.65718200	-2.72666500
O	0.98194000	2.25229300	-2.39024600	H	-0.71748400	-3.66556000	-2.75765000
H	-3.85268900	2.54257500	4.07783500	C	-3.60844500	-2.06531700	-1.95948200
C	-5.69255100	3.41095300	0.54128400	C	-4.47560900	-1.44576800	0.24797800
H	-5.50812700	3.14078100	-1.58734500	C	-3.20301100	-2.01908600	2.25208500
H	-5.62677100	3.53023600	2.68895400	H	-1.36922700	-2.99569500	2.02102100
C	2.44441900	4.14865000	-0.00080400	H	-2.71320900	-2.68606100	-3.81014800
C	1.71143000	5.57939700	-1.94151200	C	-4.75982300	-1.46021700	-2.55337000
C	0.04755100	4.18639800	-0.69187000	C	-4.35488100	-1.41938400	1.66036900
H	-6.62371200	3.96814300	0.46563100	C	-5.60404600	-0.84197900	-0.36827100
C	2.29715300	2.92654200	0.87325200	H	-3.10519300	-1.99295900	3.33666500
O	3.26991600	4.99895200	0.23598300	C	-5.71241900	-0.87009000	-1.79478300
H	1.05519200	5.63141600	-2.81747800	H	-4.84653700	-1.47834300	-3.63897900
H	2.74463500	5.70773600	-2.27360800	C	-5.34604400	-0.79836700	2.42451400
H	1.47243600	6.42496300	-1.28874800	C	-6.56849100	-0.22703800	0.43275900
H	-0.14912300	4.99412700	0.02208000	H	-6.58124900	-0.40260500	-2.25651400
H	-0.64817000	4.29741400	-1.52996200	C	-6.44036400	-0.20661700	1.81377000
H	-0.17885400	3.23106600	-0.21095400	H	-5.24014300	-0.77503500	3.50817900
C	3.63123100	2.40982800	1.37024400	H	-7.42460200	0.24758700	-0.04487400
H	1.66592200	3.21938800	1.72642200	H	-7.19882600	0.28445500	2.41944100

## Cartesian Coordinates of the optimized **13•Na<sup>+</sup>**

N	0.32821500	0.34202400	-2.74839400	C	-2.37639400	1.51612800	0.70788200
C	1.33161900	0.68488600	-1.91484900	H	-3.68502200	3.11559100	1.38388900
C	-0.71850900	-0.56303200	-2.43097500	H	-3.61967100	2.85159500	-0.34864300
H	0.25591500	0.83596700	-3.62810700	C	-3.14397800	0.45846000	1.52062200
C	2.28161300	1.79382500	-2.39334300	O	-1.29383300	1.30976600	0.21187800
O	1.49100000	0.18668100	-0.80877700	C	-2.53919500	-0.94656000	1.39885800
C	-2.04383900	-0.11376500	-2.50370000	C	-2.93794500	0.84767600	3.00316900
C	-0.42375900	-1.87589200	-2.09151400	C	-4.63599400	0.49132700	1.18562200
C	2.00233200	2.90679200	-1.36616000	C	-3.44645400	-2.13035400	1.61658500
C	1.99420000	2.33841400	-3.78809000	O	-1.34847400	-1.12799500	1.25909300
C	3.70159400	1.24075900	-2.34383500	H	-3.50346800	0.17452600	3.65684500
C	-3.08649500	-1.04916400	-2.27120300	H	-3.29451800	1.86431000	3.18807900
C	-2.39104500	1.24836000	-2.78078000	H	-1.88128900	0.80600700	3.29107700
C	-1.44045300	-2.78361700	-1.85292500	H	-4.83372200	0.20853400	0.14527500
H	0.61754500	-2.18321300	-2.03258300	H	-5.20134100	-0.18250700	1.83531700
C	2.94994400	3.11097800	-0.21703600	H	-5.05308500	1.48877700	1.34344900
O	0.99170400	3.56614100	-1.46924800	C	-2.74759100	-3.48916900	1.56588700
H	2.11986300	1.55971200	-4.54879500	H	-3.97688400	-1.97672100	2.56582700
H	2.71088900	3.13098100	-4.02786000	H	-4.24147300	-2.11900300	0.85716000
H	0.99658000	2.77916800	-3.87507100	C	-1.28005500	-3.62054500	1.91560600
H	3.80936800	0.42798100	-3.07214000	H	-3.29207400	-4.18783900	2.21788100
H	4.43608800	2.01144900	-2.60339000	H	-2.82534800	-3.89954300	0.55456900
H	3.95115900	0.83363600	-1.36334000	C	-0.72968200	-3.22892600	3.30503600
C	-2.77938600	-2.40035600	-1.96017800	O	-0.54096900	-4.18581800	1.13569000
C	-4.44394700	-0.62906100	-2.33626000	C	0.39246900	-2.19287100	3.11108100
C	-3.68470400	1.64402600	-2.84247500	C	-1.76979000	-2.66778900	4.26071000
H	-1.59972900	1.98443400	-2.90682800	C	-0.15441700	-4.51090000	3.93205400
H	-1.19661200	-3.81072600	-1.58737100	N	1.42908400	-2.61432200	2.33234500
C	2.45095400	4.19446000	0.71750500	O	0.34109900	-1.08283800	3.61335200
H	3.94876600	3.34985700	-0.60503500	H	-1.32876100	-2.53980100	5.25371200
H	3.06753200	2.14897900	0.30127200	H	-2.61239200	-3.35941200	4.36568200
C	-3.85638100	-3.32351300	-1.76251800	H	-2.14586200	-1.68867100	3.96316700
C	-4.75844200	0.72531600	-2.62070100	H	-0.96650400	-5.21652500	4.14259200
C	-5.48964100	-1.55857200	-2.09412900	H	0.56588000	-5.01591900	3.28570000
H	-3.93031700	2.68558400	-3.04617900	H	0.33757600	-4.27581600	4.88160900
C	1.12441500	3.82665900	1.33262900	C	2.54956600	-1.85193600	1.94566700
H	2.39899500	5.15822600	0.20525300	H	1.26135300	-3.48285200	1.83399300
H	3.15852500	4.32177500	1.54961400	C	3.13889000	-2.08911900	0.68671800
C	-5.14880500	-2.92240700	-1.82043300	C	3.09031300	-0.89642300	2.80665600
H	-3.61251000	-4.36740200	-1.57013800	C	4.31312500	-1.36719400	0.33883500
C	-6.09660000	1.12619400	-2.64116500	C	2.60760600	-3.01841200	-0.26547700
C	-6.81429900	-1.11488300	-2.12641400	C	4.20579100	-0.16578400	2.43854900
C	0.12373200	4.91797900	1.70701700	H	2.63564800	-0.73659800	3.77703400
O	0.88878500	2.67317400	1.63349900	C	4.84544400	-0.38926900	1.21927100
H	-5.95666000	-3.63554900	-1.66478800	C	4.95670500	-1.60582700	-0.90662600
C	-7.11206700	0.21373700	-2.39384500	C	3.21754500	-3.23409400	-1.45615200
H	-6.33367700	2.16712700	-2.85489300	H	1.68066700	-3.54944000	-0.05610300
H	-7.61490100	-1.82841700	-1.93954500	H	4.61328000	0.57393000	3.12548000
C	-1.25463200	4.24494300	1.75758900	C	6.02317000	0.32949800	0.83976500
C	0.53433100	5.38306400	3.10710800	C	4.41547100	-2.54589900	-1.81999100
C	0.09776900	6.11016200	0.75068700	C	6.13366200	-0.88940100	-1.25223100
H	-8.14861500	0.54093900	-2.41309600	H	2.79180200	-3.94163800	-2.16644900
C	-1.94035800	3.96431200	0.43638700	C	6.64533300	0.08510900	-0.33746200
O	-1.78124500	3.96588000	2.80752300	H	6.41615400	1.07336000	1.53121000
H	1.53669900	5.82481100	3.08729400	C	5.05486600	-2.75913200	-3.04455100
H	0.52593700	4.55771200	3.82342100	C	6.74279800	-1.13621900	-2.48475100
H	-0.16217700	6.14851100	3.46468600	H	7.54693700	0.62984500	-0.61277200
H	-0.74473800	6.76638800	0.99831100	C	6.20896500	-2.06238800	-3.36953800
H	1.00450700	6.71416700	0.85430300	H	4.63596600	-3.48354900	-3.74095800
H	0.00599100	5.81230500	-0.29745300	H	7.64644200	-0.58792600	-2.74578700
C	-3.00223100	2.88800100	0.56188900	H	6.69758800	-2.24151200	-4.32418000
H	-2.39942500	4.90801200	0.10854100	Na	0.57999900	0.33294100	1.32168600
H	-1.20128700	3.70861800	-0.33148900				

## 9. References

- [1] Y. Inaba, Y. Nomata, Y. Ide, J. Pirillo, Y. Hijikata, T. Yoneda, A. Osuka, J. L. Sessler, Y. Inokuma, *J. Am. Chem. Soc.*, 2021, **143**, 12355–12360.
- [2] P. D. Williams and E. LeGoff, *J. Org. Chem.* 1981, 4143–4147.
- [3] G. Cafeo, F. H. Kohnke, M. F. Paris, R. P. Nascone, G. L. La Torre, D. J. Williams, *Org. Lett.*, 2002, **4**, 2695–2697.
- [4] M. Uesaka, Y. Saito, S. Yoshioka, Y. Domoto, M. Fujita, Y. Inokuma, *Commun. Chem.*, 2018, **1**, 23.
- [5] M. G. Sheldrick, *Acta Crystallogr. Sect. A*, 2015, **71**, 3-8.
- [6] M. G. Sheldrick, *Acta Crystallogr. Sect. C*, 2015, **71**, 3-8.
- [7] J. N. Freskos, S. A. Laneman, M. L. Reilly, D. H. Rupin, *Tetrahedron Lett.*, 1994, **35**, 835–838.
- [8] Y. Niko, S. Kawauchi, S. Otsu, K. Tokumaru, G. Konishi, *J. Org. Chem.*, 2013, **78**, 3196–3207.
- [9] P. Thordarson, *Chem. Soc. Rev.*, 2011, **40**, 1305–1323.
- [10] L. Fielding, *Tetrahedron*, 2000, **56**, 6151–6170.
- [11] B. Hourahine, B. Aradi, V. Blum, F. Bonafé, A. Buccheri, C. Camacho, C. Cevallos, M. Y. Deshaye, T. Dumitrică, A. Dominguez, S. Ehlert, M. Elstner, T. van der Heide, J. Hermann, S. Irle, J. J. Kranz, C. Köhler, T. Kowalczyk, T. Kubař, I. S. Lee, V. Lutsker, R. J. Maurer, S. K. Min, I. Mitchell, C. Negre, T. A. Niehaus, A. M. N. Niklasson, A. J. Page, A. Pecchia, G. Penazzi, M. P. Persson, J. Řezáč, C. G. Sánchez, M. Sternberg, M. Stöhr, F. Stuckenbergs, A. Tkatchenko, V. W.-z. Yu, and T. Frauenheim, *J. Chem. Phys.*, 2020, **152**, 124101.
- [12] M. Gaus, A. Goez, M. Elstner, *J. Chem. Theory Comput.*, 2013, **9**, 338–354.
- [13] M. Kubillus, T. Kubař, M. Gaus, J. Řezáč, M. Elstner, *J. Chem. Theory Comput.*, 2015, **11**, 342.
- [14] S. Grimme, J. Antony, S. Ehrlich, H. Krieg, *J. Chem. Phys.*, 2010, **132**, 154104.
- [15] S. Grimme, S. Ehrlich, L. Goerigk, *J. Comput. Chem.*, 2011, **32**, 1456–1465.
- [16] S. Nosé, *J. Chem. Phys.*, 1984, **81**, 511.
- [17] W. G. Hoover, *Phys. Rev. A*, 1985, **31**, 1695–1697.
- [18] Y. Zhao, D. G. Truhlar, *Theor. Chem. Acc.*, 2008, **120**, 215–241.

- [19] E. Cancés, B. Mennucci, J. Tomasi, *J. Chem. Phys.*, 1997, **107**, 3032.
- [20] Gaussian 16, Revision C.01, M. J. Frisch, G. W. Trucks, H. B. Schlegel, G. E. Scuseria, M. A. Robb, J. R. Cheeseman, G. Scalmani, V. Barone, G. A. Petersson, H. Nakatsuji, X. Li, M. Caricato, A. V. Marenich, J. Bloino, B. G. Janesko, R. Gomperts, B. Mennucci, H. P. Hratchian, J. V. Ortiz, A. F. Izmaylov, J. L. Sonnenberg, D. Williams-Young, F. Ding, F. Lipparini, F. Egidi, J. Goings, B. Peng, A. Petrone, T. Henderson, D. Ranasinghe, V. G. Zakrzewski, J. Gao, N. Rega, G. Zheng, W. Liang, M. Hada, M. Ehara, K. Toyota, R. Fukuda, J. Hasegawa, M. Ishida, T. Nakajima, Y. Honda, O. Kitao, H. Nakai, T. Vreven, K. Throssell, J. A. Montgomery, Jr., J. E. Peralta, F. Ogliaro, M. J. Bearpark, J. J. Heyd, E. N. Brothers, K. N. Kudin, V. N. Staroverov, T. A. Keith, R. Kobayashi, J. Normand, K. Raghavachari, A. P. Rendell, J. C. Burant, S. S. Iyengar, J. Tomasi, M. Cossi, J. M. Millam, M. Klene, C. Adamo, R. Cammi, J. W. Ochterski, R. L. Martin, K. Morokuma, O. Farkas, J. B. Foresman, and D. J. Fox, Gaussian, Inc., Wallingford CT, 2016.